Final Report

FLORIDA'S WET WEATHER DEMONSTRATION PROJECT

Contract No. BDI91

Adam M. Pike, E.I.T
Paul J. Carlson, Ph.D., P.E.

Texas Transportation Institute
The Texas A&M University System
3135 TAMU
College Station, TX 77843-3135

and

Jason E. Meyer
Ronald B. Gibbons, Ph.D.

Virginia Tech Transportation Institute
3500 Transportation Research Plaza
Blacksburg, VA 24601

Prepared for:

Florida Department of Transportation
605 Suwannee Street
Tallahassee, FL 32399

January 2009

DISCLAIMER

The opinions, findings, and conclusions expressed in this publication are those of the authors and not necessarily those of the State of Florida Department of Transportation.

The Texas Transportation Institute and the authors of this report do not endorse products or manufacturers. Product or manufacturers' names appear herein solely because they are considered essential to the object of this report.

UNIT CONVERSION TABLE

Length				
inches (in)	*	25.4	=	millimeters (mm)
feet (ft)	*	0.305	=	meters (m)
yards (yd)	*	0.914	=	meters (m)
miles (m)	*	1.61	=	kilometers (km)
Area				
square inches (in^2)	*	645.2	=	square millimeters (mm^2)
square feet (ft^2)	*	0.093	=	square meters (ft^2)
Volume				
fluid ounces (fl oz)	*	29.57	=	milliliters (mL)
gallons (gal)	*	3.785	=	liters (L)
Illumination				
foot-candles (fc)	*	10.76	=	lux (lx)
foot-lamberts (fl)	*	3.426	=	candela/m^2 (cd/m^2)

TECHNICAL REPORT DOCUMENTATION PAGE

1. Report No.	2. Government Accession No.	3. Recipient's Catalog No.
4. Title and Subtitle Florida's Wet Weather Demonstration Project		5. Report Date November 2008
		6. Performing Organization Code
7. Author(s) Adam M. Pike, Paul J. Carlson, Jason E. Meyer, and Ronald B. Gibbons		8. Performing Organization Report No.
9. Performing Organization Name and Address Texas Transportation Institute The Texas A&M University System College Station, TX 77843-3135		10. Work Unit No. (TRAIS)
		11. Contract or Grant No. BDI91
12. Sponsoring Agency Name and Address Florida Department of Transportation 605 Suwannee Street, MS 30 Tallahassee, FL 32399		13. Type of Report and Period Covered Draft Final Report August 2007 – November 2008
		14. Sponsoring Agency Code
15. Supplementary Notes		

16. Abstract

The Florida Department of Transportation (FDOT) established a wet-weather pavement marking demonstration project with goals to gather performance data, evaluate various wet-weather marking systems, and develop a measurement protocol for measuring retroreflectivity under continuous wetting conditions. FDOT coordinated the installation of a variety of specially designed pavement marking systems along a section of Interstate Highway 10, just west of Tallahassee, Florida. Being a test deck designed specifically for wet-nighttime performance, most of the markings had special characteristics to provide enhanced wet-nighttime performance. The standard marking used as a control was the standard FDOT application of double drop optics (both optics having 1.5 refractive indices) on non-profiled thermoplastic.

Several continuous wetting handheld retroreflectivity measurement protocols were tested against charged coupled device (CCD) based luminance measurements. While the overall correlations were strong, it was noted that the control pavement marking system (without specially designed wet-nighttime performance characteristics) suffered from inequitable and unrepresentative measurement results under the highest continuous wetting rates. From a practical point of view, the correlations were just as strong for the lower continuous wetting rates and the measurement results of the control pavement marking system (without specially designed wet-nighttime performance characteristics) were much more equitable and representative. Therefore, the researchers recommended a measurement protocol for measuring the retroreflective performance of pavement markings systems under continuous wetting conditions that was based on a wetting rate of approximately 2 inch per hour. A complete set of guidelines is provided for the measurement protocol, including detailed drawings and a parts list for the equipment needed to implement the recommended protocol.

17. Key Word	18. Distribution Statement
Retroreflectivity, Visibility, Pavement Markings, Wet Weather, Continuous Wetting, Luminance	Unrestricted

19. Security Classif. (of this report)	20. Security Classif. (of this page)	21. No. of Pages	22. Price
Unclassified	Unclassified	112	

Form DOT F 1700.7 (8-72) Reproduction of completed page authorized

ACKNOWLEDGMENTS

This project was conducted in cooperation with the Florida Department of Transportation. The authors wish to acknowledge Chester Henson the FDOT Project Manager whose insight and assistance aided in the successful completion of the this research project.

The authors would like to acknowledge Ivan Lorenz of the Texas Transportation Institute. Ivan helped develop the continuous wetting systems used in the testing and the final recommended system. Ivan also helped collect data on the pavement marking test deck in Florida.

EXECUTIVE SUMMARY

Pavement markings are often considered to be the most valuable and important means of communicating roadway information to the driver. Longitudinal pavement markings are able to provide a continuous stream of guidance to drivers as they delineate the roadway. Traditionally, pavement marking systems have provided adequate delineation under dry nighttime conditions but have failed during wet nighttime conditions. In recent years, many pavement marking systems have been developed to provide improved delineation during wet-night weather conditions. To provide improved delineation during wet-night conditions, pavement markings must be able to retroreflect in both continuous wetting conditions and in dry conditions.

The Florida Department of Transportation (FDOT) established a wet-weather marking demonstration project with goals to gather a variety of pavement marking performance data, evaluate various wet-weather marking systems, and develop a measurement protocol for measuring retroreflectivity under continuous wetting conditions. FDOT coordinated the installation of a variety of specially designed pavement marking systems along a section of Interstate Highway 10 (I-10), just west of Tallahassee, Florida. Being a test deck designed specifically for wet-nighttime performance, most of the markings had special characteristics to provide enhanced wet-nighttime performance. The standard marking used as a control was the standard FDOT application of double drop optics (both optics having 1.5 refractive indices) on non-profiled thermoplastic.

The Texas Transportation Institute (TTI) and Virginia Tech Transportation Institute (VTTI) assisted FDOT in achieving their goals of the demonstration project. Using the latest research techniques and photometric equipment, the researchers measured the performance of the markings on the FDOT test deck, analyzed the data, and developed recommendations for continuous wetting measurement protocols for pavement markings. The recommended measurement protocols are equitable (produce unbiased results regardless of the pavement marking system) and representative (produces results that correlate with nighttime visual inspections and/or measurement protocol).

One of the unique efforts included was the comparison of handheld retroreflective measurements to charged coupled device (CCD) based retroreflective measurements. The researchers collected both sets of data in order to compare how well these different methods to measure pavement marking performance compared. The handheld method is a simple method to

implement in the field and provides a surrogate for estimated performance of the marking. The CCD photometer measurements provide more of a direct measurement of the actual performance in the field. If the handheld measurements could be correlated with the CCD measurements, then there would be validity for test methods using the easier-to-use handheld retroreflectometer.

The researchers performed several handheld measurement protocols and tested the results against the CCD-based measurements. While the overall correlations were strong, it was noted that the control pavement marking system (without specially designed wet-nighttime performance characteristics) suffered from inequitable and unrepresentative measurement results under the highest continuous wetting rates. From a practical point of view, the correlations were just as strong for the lower continuous wetting rates and the measurement results of the control pavement marking system (without specially designed wet-nighttime performance characteristics) were much more equitable and representative. Therefore, the researchers recommended a measurement protocol for measuring the retroreflective performance of pavement markings systems under continuous wetting conditions that was based on a wetting rate of approximately 2 inch per hour. A complete set of guidelines is provided for the measurement protocol, including detailed drawings and a parts list for the equipment needed to implement the recommended protocol.

TABLE OF CONTENTS

Page

LIST OF FIGURES

Page

LIST OF TABLES

Page

CHAPTER 1: INTRODUCTION

Pavement markings are often considered to be the most valuable and important means of communicating roadway information to the driver. Longitudinal pavement markings are able to provide a continuous stream of guidance to drivers as they delineate the roadway. Traditionally, pavement marking systems have provided adequate delineation under dry nighttime conditions but have failed during wet-nighttime conditions. In recent years, many pavement marking systems have been developed to provide improved delineation during wet-night weather conditions. To provide improved delineation during wet-night conditions, pavement markings must be able to retroreflect in both continuous wetting conditions and in dry conditions.

The Florida Department of Transportation (FDOT) established a wet-weather marking demonstration project and invited participation from all pavement marking manufacturers that had a wet-weather pavement marking system. Various wet-weather markings were installed as well as a standard FDOT marking as a control section. The demonstration project test area is on I-10 west of Tallahassee, Florida. The demonstration facility is a four-lane divided highway, composed of an open-graded friction course road surface with concrete bridges. The posted speed limit is 70 miles per hour. The traffic volume is approximately 9400 vehicles/lane/day, and is composed of approximately 20 percent trucks. Each pavement marking system was applied to a one-quarter mile segment of the demonstration project. All lines in the test area were required to be applied with each wet-weather pavement marking system, which is the left yellow edgeline, the white lane line, and the outside white edgeline.

The goals of the demonstration project were to gather a variety of pavement marking performance data, evaluate various wet-weather marking systems, and develop recommendations for a wet-weather marking specification. The wet-weather marking specification would require the development of a measurement protocol for wet-retroreflectivity of longitudinal pavement markings. This measurement protocol would need to be equitable (produce unbiased results regardless of the pavement marking system) and representative (produces results that correlate with nighttime visual inspections and/or measurement protocol) to establish wet-retroreflectivity requirements for pavement markings.

It was anticipated that this research would lead to a measurement protocol similar to that of ASTM E2176, but with a lower rate of continuous wetting. The current rate of continuous wetting is over 9 inches per hour (iph) which floods conventional markings. The resulting

retroreflectivity measurements have been shown to be inequitable and unrepresentative when compared to visibility assessments in typical rain conditions. A reason often claimed but not formally referenced for the high rainfall rate of 2176 is to account for the transmission of light loss through 30 meters of rain. To study the effect of rain on light transmission, transmissivity of various simulated rainfall rates were also studied.

The Texas Transportation Institute (TTI) and Virginia Tech Transportation Institute (VTTI) assisted FDOT in achieving their goals of the demonstration project. The research included two phases. In the first phase, the research team developed and analyzed transmissivity curves for a variety of rainfall intensities. This work was completed at the TTI and VTTI rain ranges. Appendix A describes the work from the first phase. In the second phase, both TTI and VTTI collected and analyzed pavement marking performance data at the I-10 test sites. The main body of this report describes work from the second phase. The results of these efforts were used to develop a continuous wetting measurement protocol for FDOT. Appendix B and C describe the measurement protocol. The recommended measurement protocol was also presented to ASTM and is being balloted for adoption as a new ASTM test method.

CHAPTER 2: METHODOLOGY

This chapter describes the method of data collection on the pavement markings that were installed on the I-10 test deck west of Tallahassee Florida. The research team collected the following data on the I-10 test deck: dry retroreflectivity, reflected luminance for standard condition of wetness (recovery, ASTM 2177), reflected luminance for continuous wetting, daytime chromaticity, nighttime chromaticity, and illuminance and luminance using a standard light source with a CCD photometer. The data collection took place during the week of September 10, 2007.

The I-10 test deck consisted of approximately 1.5 miles of four-lane divided interstate. There were ten different products on the test deck. Each product was installed along a quarter-mile section of a single direction of travel and consists of the inside yellow edgeline, the white lane line and the outside white edgeline.

The following list describes the sequence of the marking types and location along the test deck. There were four sections heading eastbound and six sections heading westbound. Other sections that do not have test markings are also indicated for numbering purposes. Each section had the marking type, manufacturer, and any specific details listed.

Westbound:

Section 1: Pride Enterprises
All Weather Paint
Asphalt Test Section

Section 2: 3M
Polyurea Edge Lines & 380WR Tape Lane Lines
Concrete Bridge Test Section

Section 3: 3M
All Weather Paint over Thermoplastic
Asphalt Test Section

Section 4: RainLine
Inverted Rib Profile Thermoplastic
Asphalt Test Section

Section 5: 3M
380 WR ES Tape
Asphalt (a) and Concrete (b) Test Section

Section 6: Ennis Paint
Profiled Thermoplastic
Asphalt Section

Section 7: Open
Asphalt Section

Eastbound:

Section 8: Open
Asphalt Section

Section 9: Gulf Industries
Inverted Rib Profile Thermoplastic
Asphalt Test Section

Section 10: Open
Concrete & Asphalt Test Section

Section 11: Ameriseal
Profiled Thermoplastic
Asphalt Test Section

Section 12: Ameriseal
Florida Thermoplastic w/High Index & Type 4 Beads
Asphalt Test Section

Section 13: Open
Concrete Bridge Test Section

Section 14: FDOT
Florida Double Drop Thermoplastic w/Type 1 & Type 4 Beads
Asphalt Test Section

A lane closure provided by FDOT allowed for data collection throughout the day and night. The daytime lane closure began at 9 a.m. and lasted until 4 p.m. The nighttime lane closure began at 9 p.m. and generally lasted until about 3 a.m. During the day, the research team collected dry retroreflectivity, retroreflectivity in a standard condition of wetness (recovery, ASTM 2177), retroreflectivity during continuous wetting, daytime chromaticity, and nighttime chromaticity. All of these measurements can be conducted in either day or night conditions. The data collection that was not completed during the day was completed during the night data collection period. During the night data collection period the research team focused on collecting illuminance and luminance data. The luminance data collection technique can only be conducted at night. The research team collected illuminance and luminance data in dry and continuous wetting conditions.

The data collection protocol was designed to yield enough data to get an accurate representation of the pavement markings while keeping the data collection time within the allotted lane closure windows. The data collection protocol for this project was modeled after that described in ASTM D 6359 (*1*). Due to the length of the pavement marking test sections only the center portion was evaluated for each condition. A data collection area the length of 16 lane lines (610 feet), which is approximately half the length of the test deck, was evaluated for

each marking. There are four different protocols for the data collection. Each of these protocols relates to the different measurement conditions. All dry and color measurements followed one unique protocol, recovery measurements followed their own unique protocol, continuous wetting measurements followed a different unique protocol, and illuminance and luminance readings followed yet another unique data collection protocol. The following sections describe each of the protocols in detail.

DRY DATA COLLECTION

Dry retroreflectivity, nighttime chromaticity, and daytime chromaticity were measured using the same protocol in a dry condition. All measurements and devices met ASTM standards (*2*, *3*). Dry retroreflectivity and nighttime chromaticity were measured using an LTL-Y retroreflectometer and daytime color was measured using a BYK-Gardner color-guide. The LTL-Y measures the nighttime color of the marking at 30-meter geometry. The BYK-Gardner color-guide was set to measure daytime color using illuminant D65 with a 2° standard observer. Measurement locations for the dry readings on the edgelines were adjacent to the beginning and end of each lane line. Measurement locations on the lane lines were at the 1/3 and 2/3 points of each line. The measurements were conducted adjacent to and on each of the 16 lane lines in the data collection area. Color readings were only taken at the points adjacent to the end of the lane lines and on the 2/3 point of the lane lines. When measuring the left side of the road the readings went from the edgeline to the lane line then back to the edgeline progressing down the road in this manner. This method allowed the wet measurements to follow in a similar fashion without wetting the markings prior to dry evaluation. See Figure 1 below for further explanation of the dry data collection evaluation.

A team of two or three people conducted the dry retroreflectivity, nighttime color, and daytime color readings. One member used the retroreflectometer or color-guide to take the measurements of the marking and the other recorded the readings. A total of 32 dry retroreflectivity measurements and 16 measurements for both day and night color were made on each of the three markings (yellow edgeline, lane line, white edgeline) in each of the test sections. Appendix D Table 8, Table 9, Table 10, and Table 11 provide an example of the data collection sheets used to record the data for all lines and for both instruments.

Dry Data Collection Order of Evaluation

Yellow left edge and white skips will be measured at the same time. * White edge will be measured when traffic is on the other side of the road. Data collection will progress through all the test section on one side of the road before switching traffic pattern. Measurements on the edgelines are to be made adjacent to the beginning and end of the skip lines, and at the 1/3 and 2/3 point on the skip line. Data collection duration is approximately 1 hour per section.

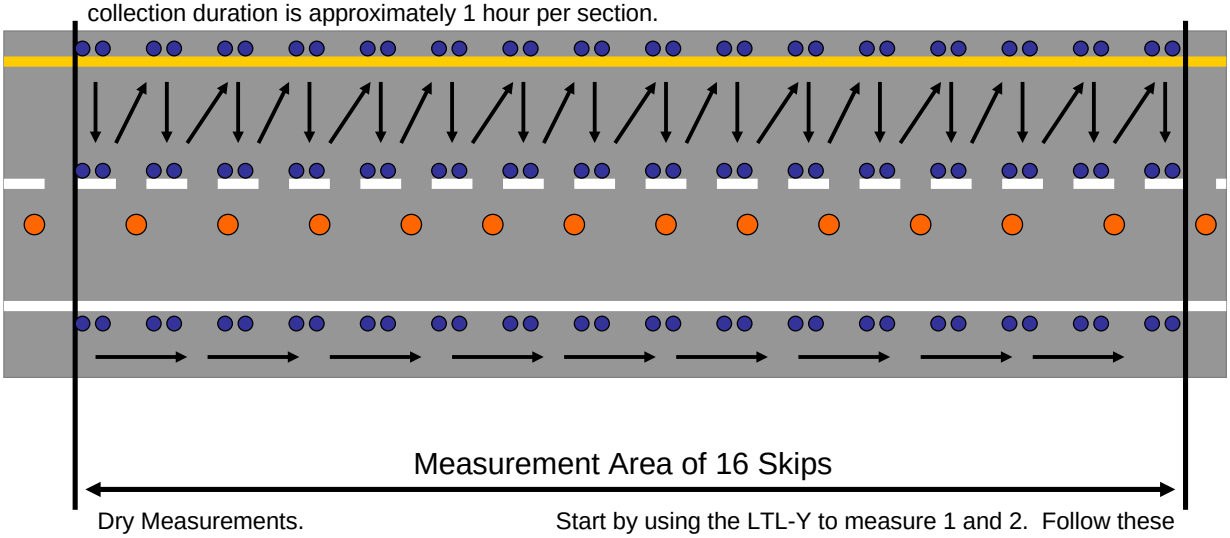

Dry Measurements.

1. Retroreflectivity, LTL-Y
2. Nighttime Chromaticity, LTL-Y
3. Daytime Chromaticity, BYK Color-guide

Start by using the LTL-Y to measure 1 and 2. Follow these measurements with the BYK color-guide to get 3. Move to the next location following the order of the arrows.

Figure 1. Dry Data Collection Order of Evaluation.

RECOVERY DATA COLLECTION

Retroreflectivity in a standard condition of wetness (recovery, ASTM 2177 [*4*]) was measured using a protocol similar to the dry measurements but not as much data were collected due to the length of time required for each individual measurement. Recovery retroreflectivity was measured using an LTL-X retroreflectometer. Measurement locations for the recovery readings on the edgelines were adjacent to the end of each lane line. Measurement locations on the lane lines were at the 2/3 point of each line. The measurements were conducted adjacent to and on each of the 16 lane lines in the data collection area. When measuring the left side of the road readings went from the edgeline to the lane line then back to the edgeline progressing down the road in this manner. This method produced the most time efficient data collection. See Figure 2 below for further explanation of the recovery data collection evaluation.

A team of two or more people conducted the recovery retroreflectivity readings. The team coordinated getting the water to pour on the line, pouring the water on the line, keeping track of the time since the water was poured, making the retroreflectivity reading, and recording the readings. Approximately 0.5-1.3 gallons of water was poured on approximately a 2 to 3 foot length of marking and the surrounding area. After the water was poured, 45 seconds were allowed to pass prior to taking the retroreflectivity measurement in the wetted area. A total of 16 measurements were made on each of the three markings (yellow edgeline, lane line, white edgeline) in each of the test sections. Appendix D Table 12 provides an example of the data collection sheets used to record the data for all lines.

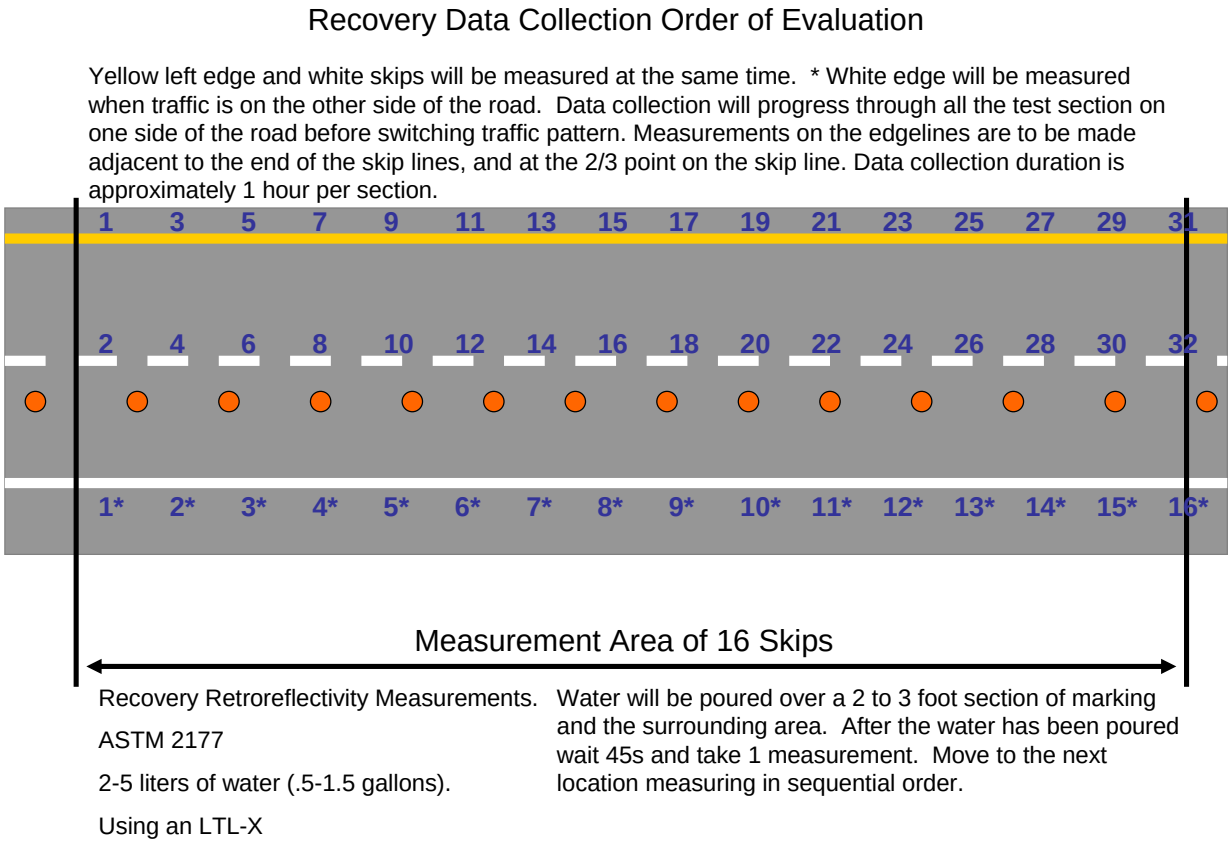

Figure 2. Recovery Data Collection Order of Evaluation.

CONTINUOUS WETTING DATA COLLECTION

Continuous wetting retroreflectivity was measured using a protocol similar to the recovery measurements but not as much data were collected due to the length of time required for each individual measurement. Continuous wetting retroreflectivity was measured using an LTL-X retroreflectometer, and a specifically designed spray rig that produces multiple levels of uniform wetting and also shields the spray area from wind to help reduce variability that wind may cause on the spray. Figure 3 shows the continuous wetting setup. A truck was used to transport the spray box, water tank, pump, and controller between each measurement location. The switch on the controller along with a single valve allowed for changing the continuous wetting rate. The metal shield surrounding the spray heads was to prevent wind from blowing the water as it sprays. Due to somewhat windy conditions, a top was added to the box shortly

after data collection began to keep the wind from swirling inside. The black paint on the lower front portion of the box was to prevent reflection of light during the CCD measurements.

Figure 3. Continuous Wetting Setup.

Measurement locations for the recovery readings on the edgelines were adjacent to the end of each lane line. Measurement locations on the lane lines were at the 2/3 point of each line. The measurements were conducted adjacent to and on only select lane lines along each test section. Measurements were made on the edgelines adjacent to lane lines 1, 4, 7, 10, 13, and 16. Measurements were made on lane lines 1, 7, and 13. When measuring the left side of the road, readings went from the edgeline to the lane line then back to the edgeline progressing down the road in this manner. This method produced the most time efficient data collection. See Figure 4 below for further explanation of the continuous wetting data collection evaluation.

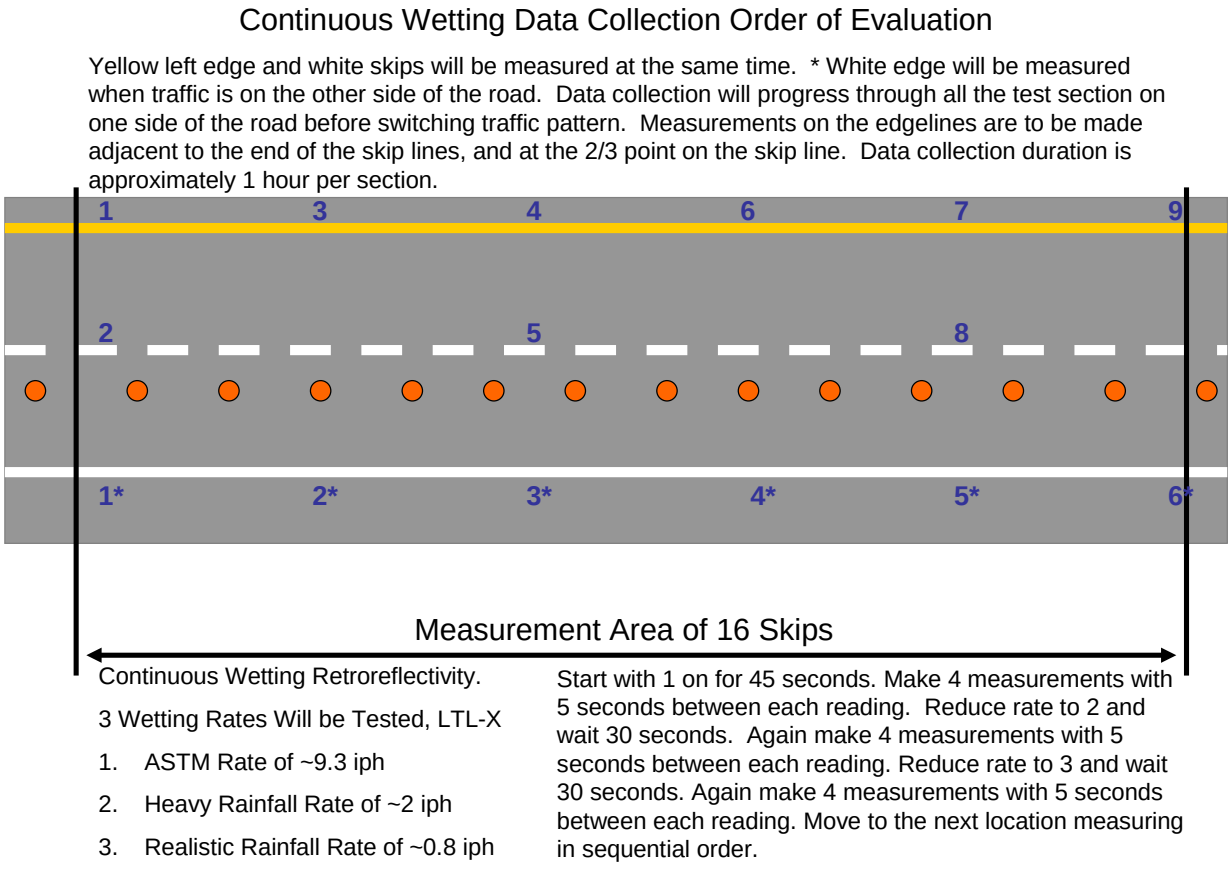

Figure 4. Continuous Wetting Data Collection Order of Evaluation.

A team of at least three people conducted the continuous wetting retroreflectivity readings (see Figure 5 for an example of the continuous wetting measurements taking place). The team coordinated getting the water sprayed on the line, making sure the spray setup was functioning properly, keeping track of the time since the water spray started and between measurements, making the retroreflectivity readings, and recording the readings. Three continuous wetting rates were tested, 9.5 inches per hour, 2.1 inches per hour, and 0.8 inches per hour. These continuous wetting rates were selected because 9.5 inches per hour is the current ASTM rate (5), 2.1 inches per hour was specified by FDOT, and 0.8 inches per hour represents a common and heavy rainfall rate. The method used for conducting the continuous wetting measurements is described in the following steps:

1. Properly align the spray unit over the marking.
2. Turn on the 9.5 iph wetting rate and let it run for 45 seconds.
3. After the 45 seconds take 4 readings with a couple of seconds between each reading.

4. Reduce the wetting rate to 2.1 iph and let it run for 30 seconds.
5. After the 30 seconds take 4 readings with a couple of seconds between each reading.
6. Reduce the wetting rate to 0.8 iph and let it run for 30 seconds.
7. After the 30 seconds take 4 readings with a couple of seconds between each reading.
8. Move to the next location and repeat making sure to record data after every measurement.

A total of six locations were measured on each edgeline and three locations on the lane lines. With four measurements recorded at each location a total of 24 measurements on each edgeline and 12 measurements on the lane lines were recorded for each of the three continuous wetting rates. Appendix D Table 13 and Table 14 provide an example of the data collection sheets for all lines.

Figure 5. Continuous Wetting Data Collection.

CCD LUMINANCE DATA COLLECTION

Luminance of the markings was measured using the CCD photometer at the same locations where the continuous wetting measurements were conducted. Only the yellow and white edgelines were measured using the CCD photometer. The lane lines were not measured due to safety concerns of taking these readings next to an open lane of traffic. Dry and continuous wetting measurements were made at each location. Dry measurements were conducted first, followed by the continuous wetting measurements. The continuous wetting

measurements were conducted by spraying water over a sufficiently large area of the marking and a CCD image being recorded while the water was being sprayed. The same continuous wetting apparatus for the retroreflectivity readings was used for the CCD readings. The CCD photometer was focused on the marking through the opening in the side of the spray box; this is the same opening that allowed the retroreflectometer to take readings while the marking was being sprayed. The CCD photometer apparatus consisted of a cart holding the CCD photometer, a computer to control the camera, and a single beam halogen headlight acting as the standard light source (the cart and the lamp were position directly above the pavement marking of interest). The distance between the camera and the light source and the distance to measurement point on the marking all complied with the 30-meter geometry that is the standard retroreflectivity measuring geometry. Data were collected in a similar manner as during the day time data collection. Since the road was still open to traffic, the researchers attempted to only take readings in the gaps between the vehicles to reduce ambient light in the measurement area. All overhead lighting in the area that may affect the measurements was turned off by FDOT prior to data collection beginning. Illuminance readings using a Minolta T-10 illuminance meter were also taken at each location. The combination of the luminance and illuminance readings allowed the researchers to back calculate retroreflective levels of the markings.

DATA COLLECTION SUMMARY NOTES

Day 1 data collection on the eastbound test sections got off to a late start due to a morning rain shower. In the meantime, a kickoff coordination meeting at the local FDOT office allowed time for the markings to dry. Daytime data collection was conducted until a second rain shower ended data collection. The goal was to try and use the nighttime data collection period to makeup for the reduced amount of daytime data collection. Nighttime data collection was also cut short due to a late night rain shower, and thus data collection on the eastbound side was not completed in the first day. CCD luminance measurements and continuous wetting measurements remained on the edgeline of two sections and recovery measurements remained on the edgeline of three sections.

Day 2 data collection started on time and was progressing on schedule until it was once again cut short due to rain. At this point it was realized that data collection was not going to be able to be completed in two days as originally planned. An extra day was added to the data

collection schedule to complete the eastbound side. The night data collection went as planned completing all the measurements on the yellow edgeline and white lane line. This left all measurements on the westbound white edgeline to be completed as well as the remaining data on the eastbound side.

Day 3 was the only day and night with no rain. Data collection progressed as planned. All the data on the westbound white edgeline was obtained during the day except for the CCD readings. That night the CCD readings were completed as well as the remaining data on the eastbound side.

ADDITIONAL/EXCLUDED DATA

An additional continuous wetting location for the lane line was included on the concrete bridge portion of Section 5. This was added to balance the number of readings on the lane lines between asphalt and concrete.

No continuous wetting measurements were conducted on the lane lines of Section 11 or 12. The rain situation forced data collection to stop prior to completing these sections during the day, and it was deemed to be too unsafe to do the data collection on the lane lines during the night. Also, as indicated in the section notes below, the lane lines in these sections had ponding issues due to the slope of the road and the location of the pavement markings.

SECTION NOTES FROM DATA COLLECTION

The following details notes from the data collection.

- Section 2: Water was ponding on areas of the white edgeline.
- Section 3: Water was ponding on yellow edgeline in areas where there was more open aggregate as opposed to tightly packed aggregate.
- Section 5: Several areas of low retroreflectivity on the white edgeline on the concrete portion of the test section. The wear was somewhat uneven across the marking as well as along the markings length. (see Figure 6 below)
- Section 11: Water was ponding along much of the lane line.
- Section 12: Water was ponding along much of the lane line.
- Section 14: Water was ponding at the end of the section on the white edgeline.

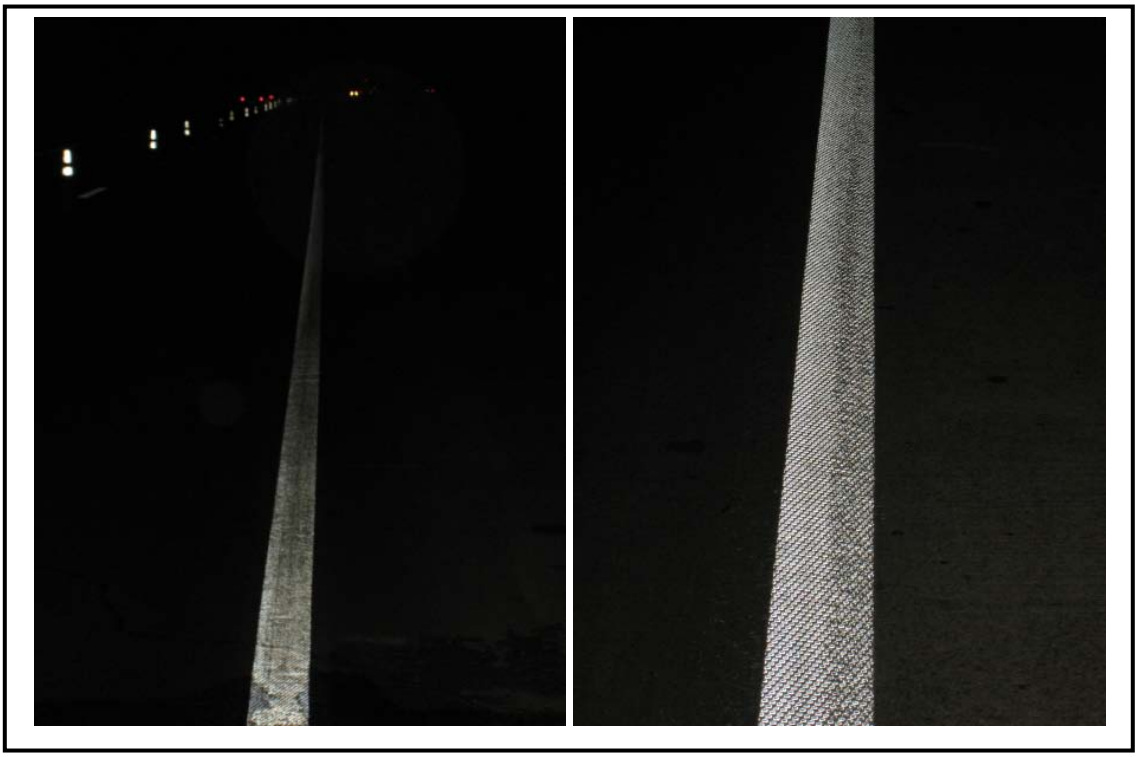

Figure 6. Uneven Wear on Section 5 Westbound Tape.

CHAPTER 3: FINDINGS

Once all the measurements were made on the test deck in Florida, the researchers prepared the data for analysis. The retroreflectivity data for dry, recovery and the three continuous wetting rates were compared to each other to see the effect of the different measurement conditions and the impact of the different continuous wetting rates. The nighttime 30-meter color measurements and the daytime D65 2° color measurements for each section were compared to the ASTM color boxes to see if the markings were meeting the necessary colors. The CCD photometer measurements, which measured the luminance of the markings in the various conditions in combination with illuminance measurements at the same locations, were used to calculate the retroreflectivity of the markings. This calculated retroreflectivity value was compared across the different measurement conditions and compared to the measured retroreflectivity values collected using the handheld retroreflectometers. This chapter describes all the data collected and the summary analysis.

RETROREFLECTIVITY DATA

The retroreflectivity data were summarized into average values for each measurement condition, for each line type, and for each marking section. Table 15 of Appendix E contains the summarized data. In addition to the average retroreflectivity values, the standard deviations of the measurements are also included in Table 15 of Appendix E. Overall the standard deviations appeared reasonable, with the exception of Section 5b. The white edgeline had relatively large standard deviations as compared to the magnitude of the average retroreflectivity values. This large standard deviation was due to the uneven wear that was noted in the previous chapter and shown in Figure 6.

The retroreflectivity values from Table 15 in Appendix E are shown in Figure 7, Figure 8, and Figure 9. Figure 7 shows the white edgeline average retroreflectivity measurements. Figure 8 shows the lane line average retroreflectivity measurements. Figure 9 shows the yellow edgeline average retroreflectivity measurements. In each figure the retroreflectivity values for all five measurement conditions are shown for each section. The figures allow for a visual comparison of the differences between the measurement conditions and between the different products.

The data indicate that as the continuous wetting rate increases the retroreflectivity typically decreases. Also in most situations the recovery retroreflectivity value is higher than the lowest continuous wetting rate, and the dry retroreflectivity reading is the highest of any condition. There are some exceptions as certain products are not impacted as much by the low continuous wetting rate. The drop in retroreflectivity between dry and wet conditions is much larger in some products than it is in others. This is due to the how the different marking systems handle the water. Some products have different types of glass beads (size or refractive index), some have structured bead systems, and some have a profiled binder to help keep the beads above the water.

Beyond the retroreflectivity performance of the markings, the color of the markings must also meet specifications. The next two sections in this chapter describe the day and night color of the marking systems. Other things to consider when evaluating pavement marking systems are the durability of the system (how long it will provide adequate performance), the installation and life cycle cost of the marking system, and any special conditions for installation, restriping, or removal.

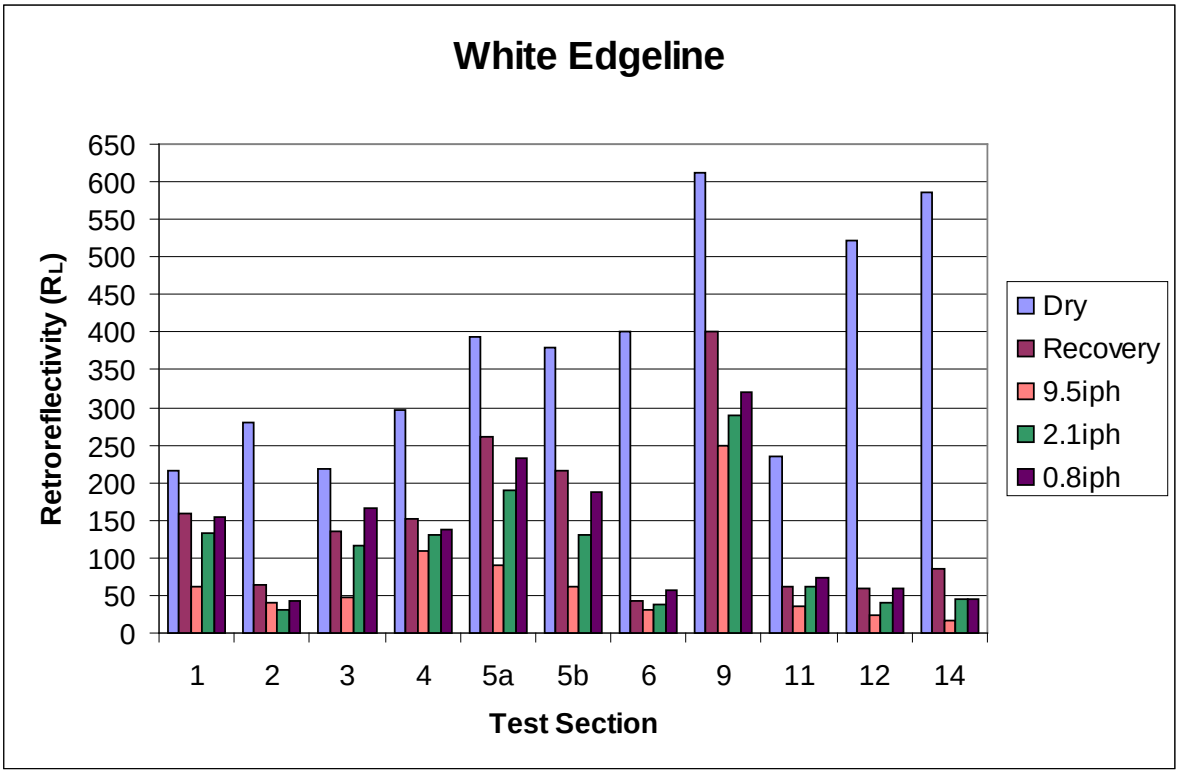

Figure 7. All Retroreflectivity Readings from All White Edgelines.

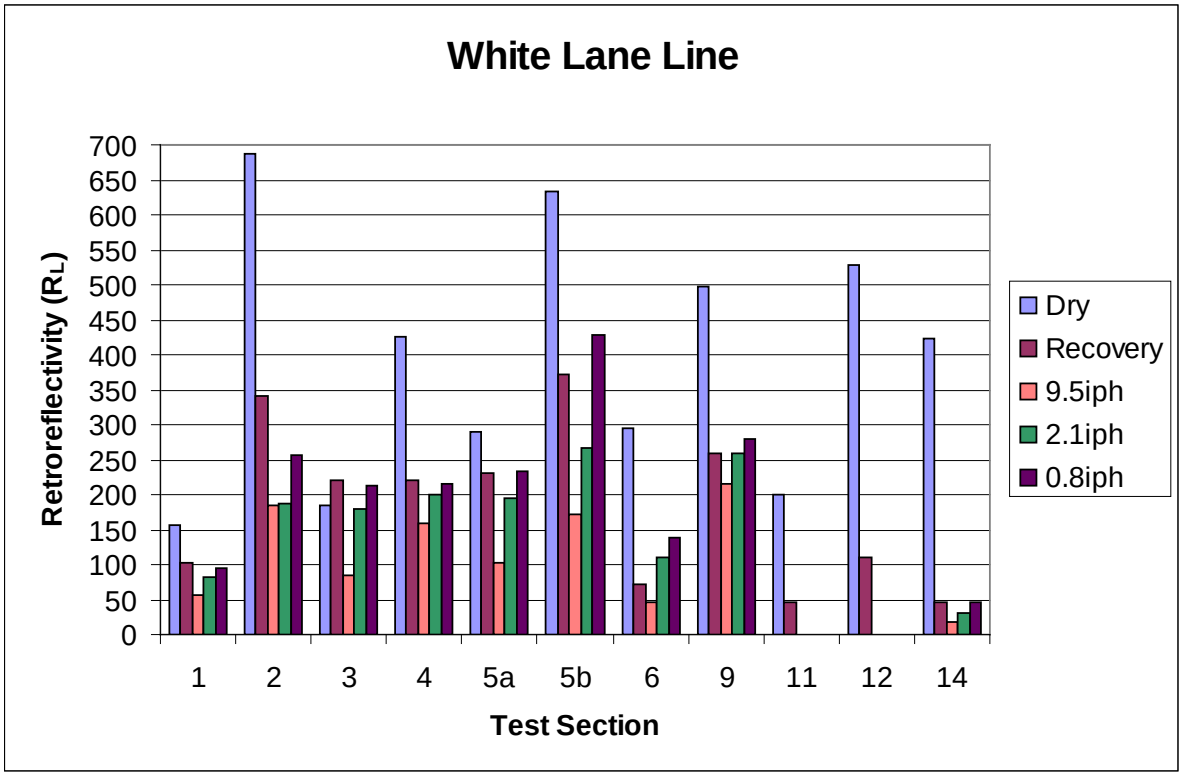

Figure 8. All Retroreflectivity Readings from All White Lane Lines.

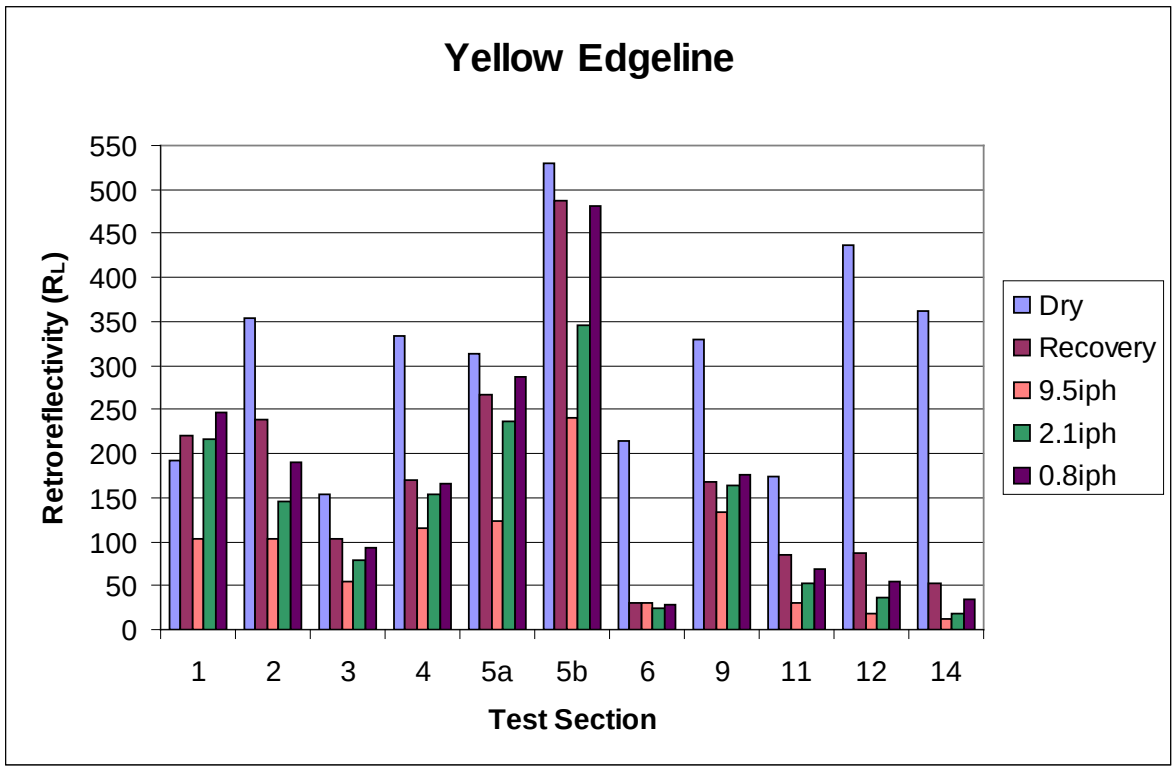

Figure 9. All Retroreflectivity Readings from All Yellow Edgelines.

CHROMATICITY DATA

Nighttime

The nighttime colors of each section and of each line were plotted on color charts with the ASTM color boxes to see if the marking color is acceptable. Every section had similar color results with the average color reading being within the color box. Several sections did have a single outlier reading not falling within the color box. The outliers could have been caused by several things including measurement error, and/or discoloration of the marking at the measurement location. Since the data for all the sections were similar, only the data for Section 14 are presented. Figure 10 shows the white edgeline readings, Figure 11 shows the lane line readings, and Figure 12 shows the yellow edgeline readings. As can be seen in these figures, there is one outlier in the lane line readings, and all other readings are within the color boxes.

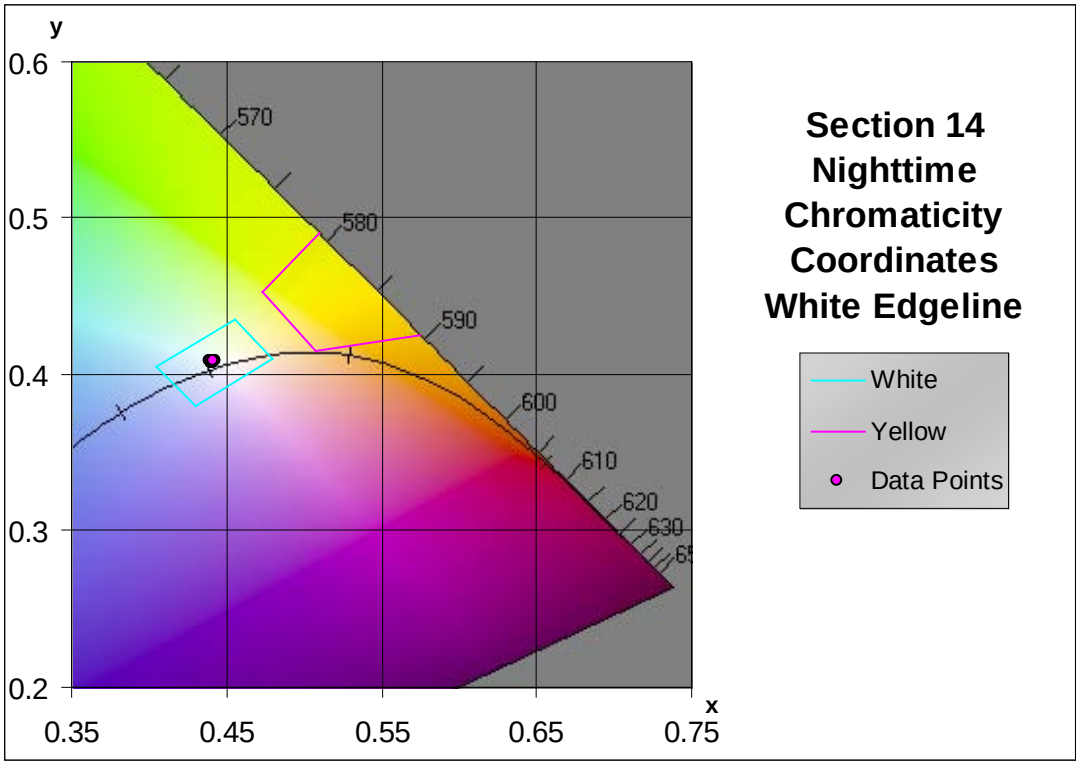

Figure 10. Section 14 White Edgeline Nighttime Color Readings.

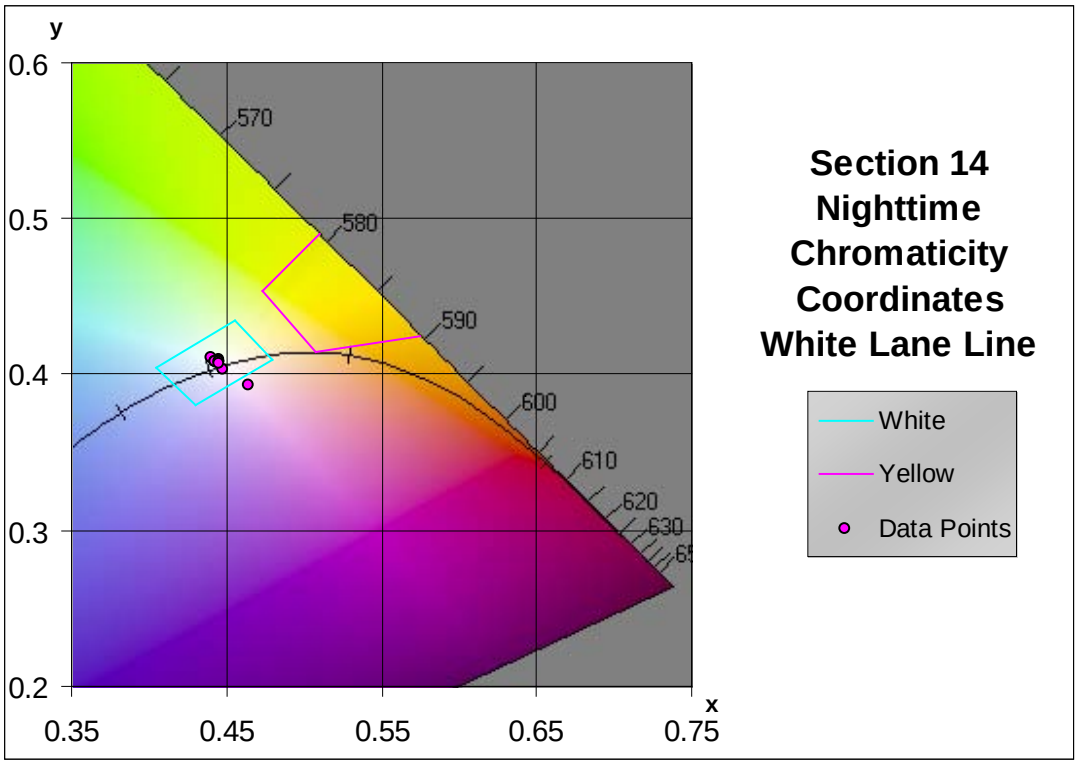

Figure 11. Section 14 White Lane Line Nighttime Color Readings.

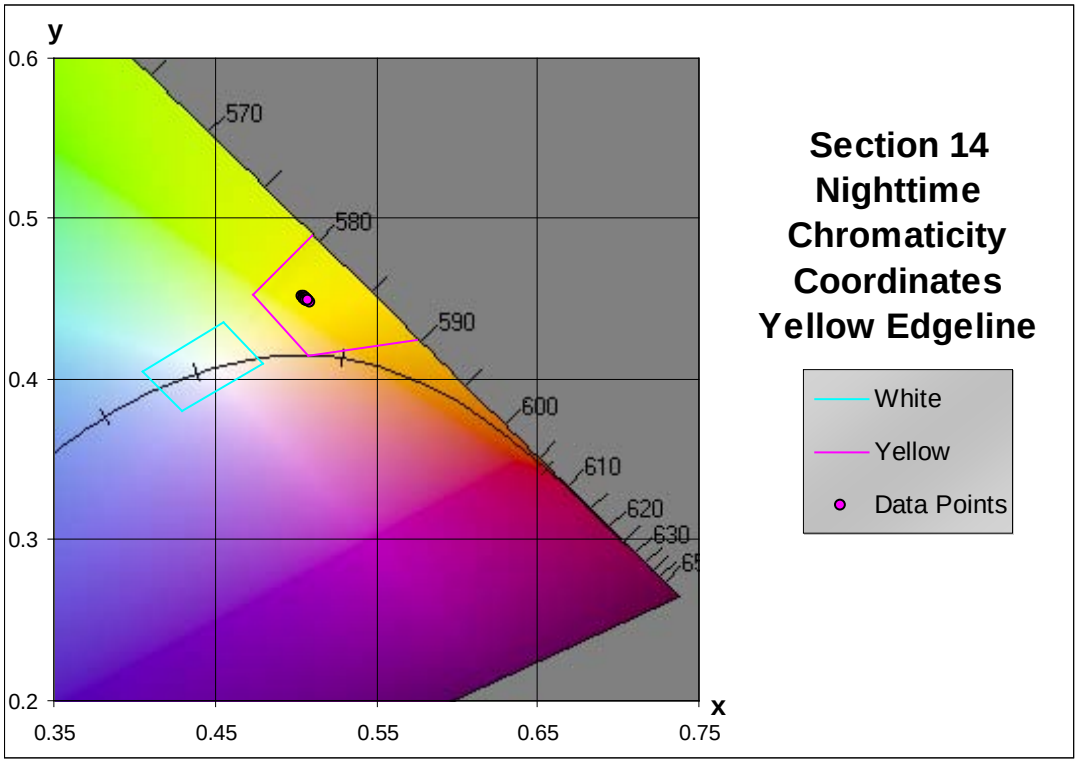

Figure 12. Section 14 Yellow Edgeline Nighttime Color Readings.

Daytime

The daytime colors of each section and of each line were plotted on charts with the ASTM color boxes to see if the marking color is acceptable. Just like the nighttime color data, every section had similar color results with the average color reading being within the color box. Several sections did have one outlier reading that did not fall within the color box. The outliers could have been caused by several things including measurement error, and/or discoloration of the marking at the measurement location. Since the data for all the sections were similar only the data for Section 14 are presented. Figure 13 shows the white edgeline readings, Figure 14 shows the lane line readings, and Figure 15 shows the yellow edgeline readings. As can be seen in these figures, all the color readings are within the color boxes.

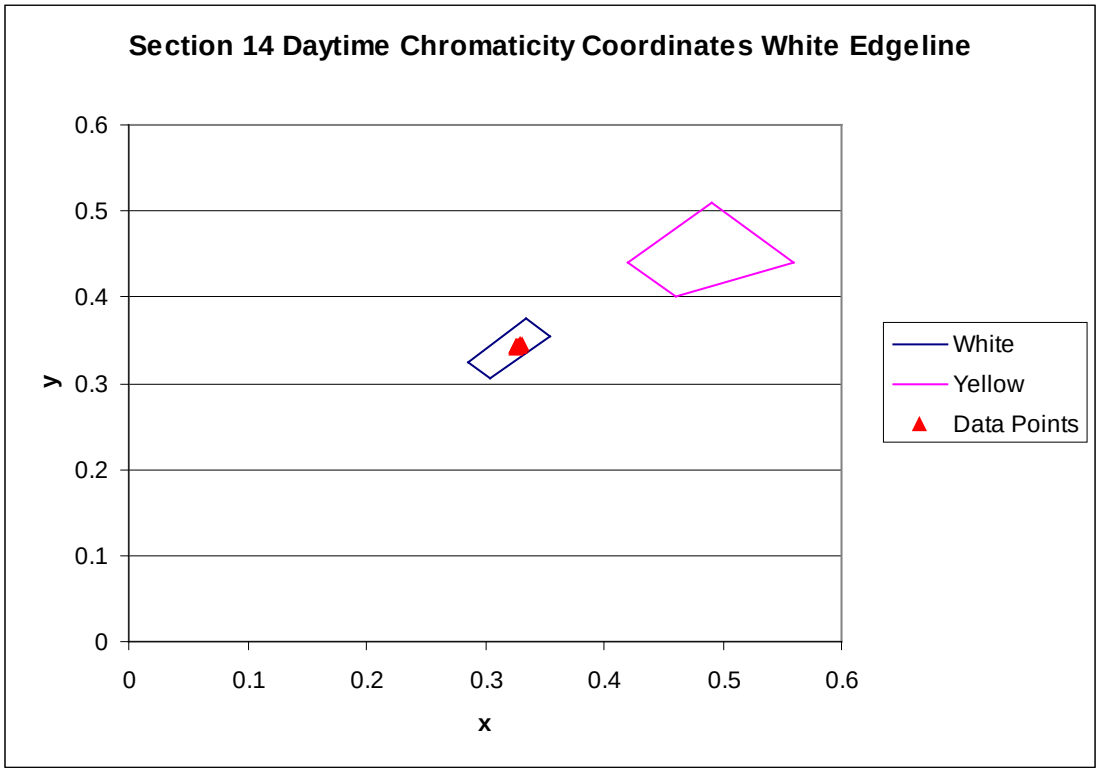

Figure 13. Section 14 White Edgeline Daytime Color Readings.

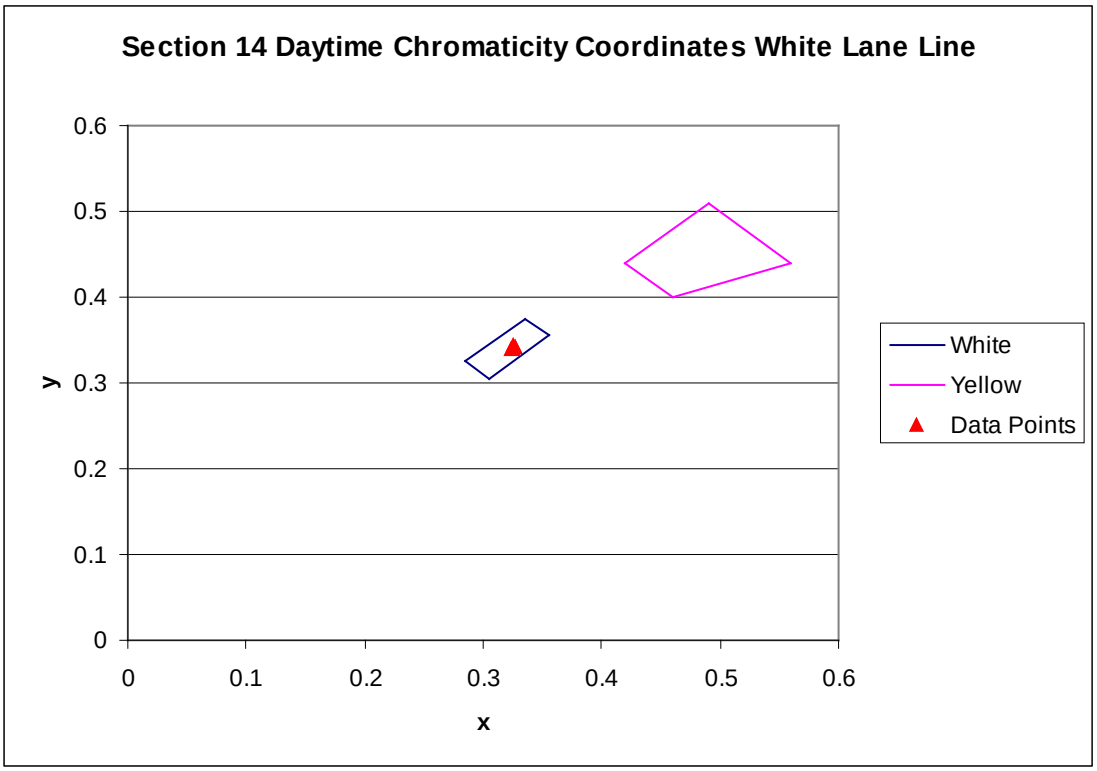

Figure 14. Section 14 White Lane Line Nighttime Color Readings.

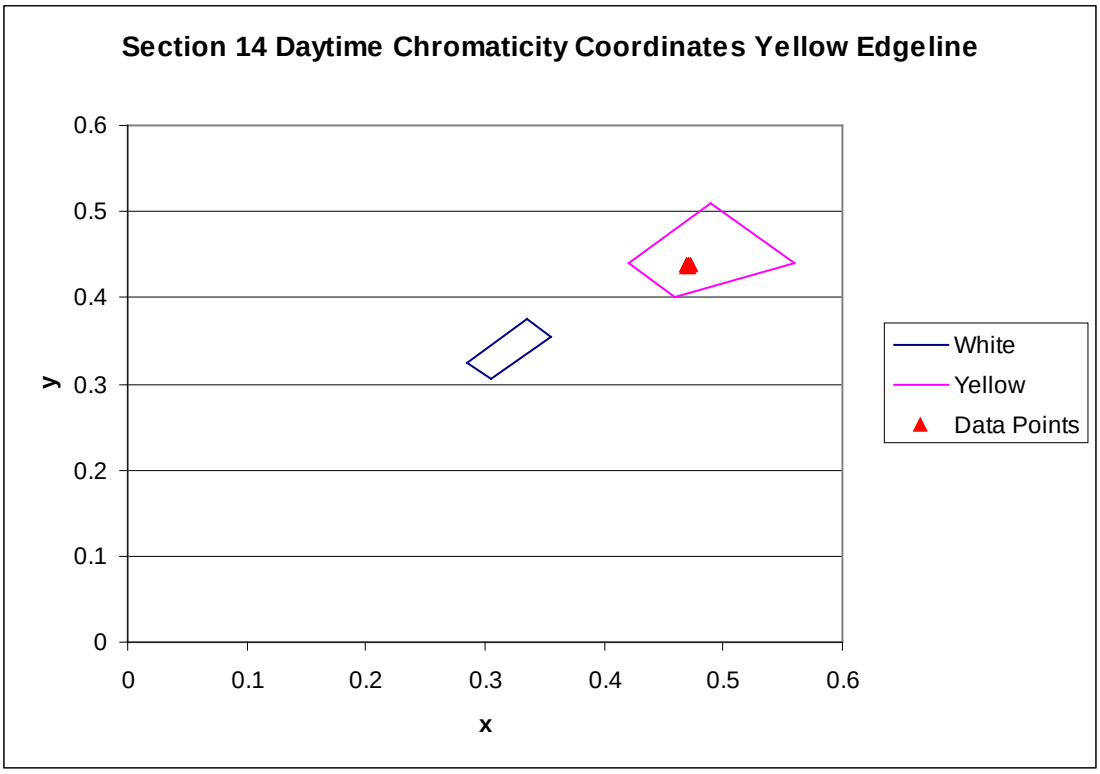

Figure 15. Section 14 Yellow Edgeline Nighttime Color Readings.

CCD PHOTOMETER MEASUREMENTS

Table 16 of Appendix F contains the summarized CCD photometer luminance measurements and the illuminance measurements. Also included in the table are the calculated retroreflectivity values of the markings based on the measured luminance and illuminance values. Illuminance is measured in lux, and luminance is measured in candelas per square meter. Retroreflectivity is a measure of the ratio of the luminance to the illuminance in millicandelas per square meter per lux. To get the calculated retroreflectivity use the equation below.

Retroreflectivity = Luminance/Illuminance*1000

Figure 16 shows the calculated retroreflectivity for the white edgeline in each section for each of the measurement conditions. Figure 17 shows the ratio of the continuous wetting retroreflectivities as compared to the dry retroreflectivity condition for the white edgeline in each section. Figure 18 shows the calculated retroreflectivity for the yellow edgeline in each section for each of the measurement conditions. Figure 19 shows the ratio of the continuous wetting retroreflectivities as compared to the dry retroreflectivity condition for the yellow edgeline in each section.

These four figures provide similar trends that were found in the retroreflectivity measurements using the handheld retroreflectometers. Typically the dry retroreflectivity is the highest and as the continuous wetting rate increases, the retroreflectivity decreases. The retroreflectivity ratios indicate how much of an impact the continuous wetting has from the dry condition. Some products retroreflectivity is impacted more than others when measured in continuous wetting conditions. The retroreflectivity ratio does not necessarily indicate which markings perform best in continuous wetting conditions but rather which markings perform closets to their dry conditions. Markings that have high dry retroreflectivity may have a low dry to continuous wetting retroreflectivity ratio but may still have an adequate continuous wetting retroreflectivity. Whereas, markings with a low dry retroreflectivity may have a high ratio but an inadequate continuous wetting retroreflectivity.

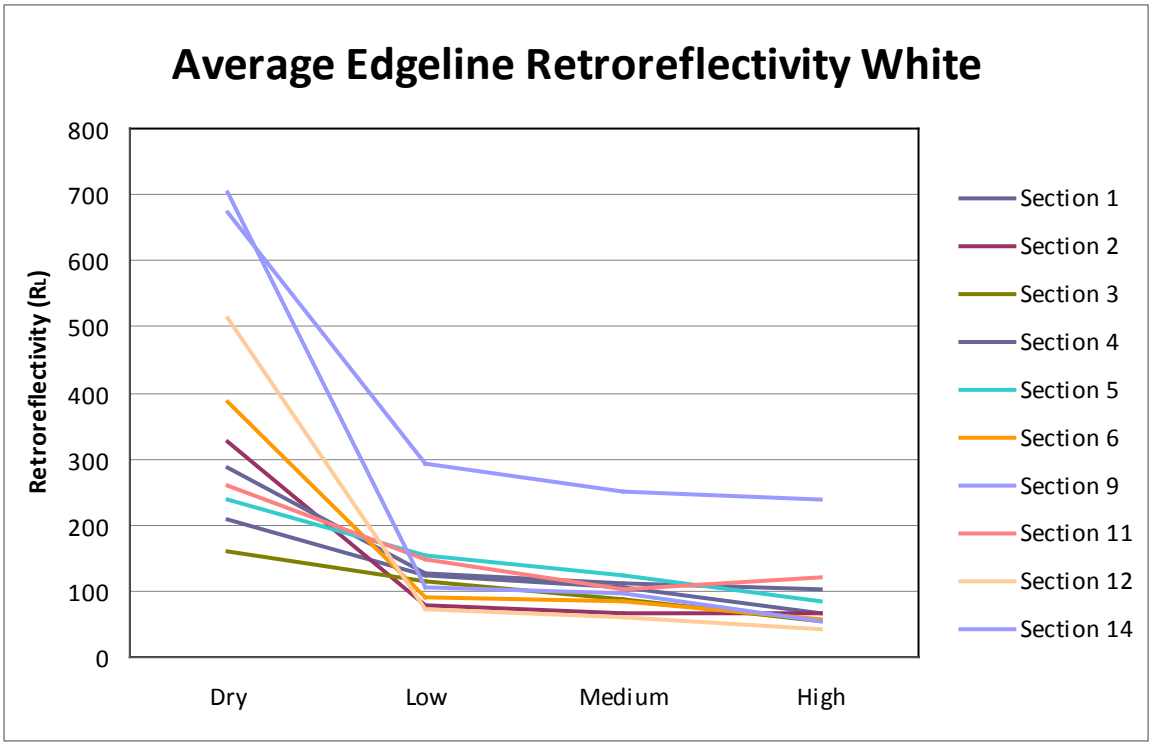

Figure 16. Average White Edgeline Retroreflectivity from CCD Measurements.

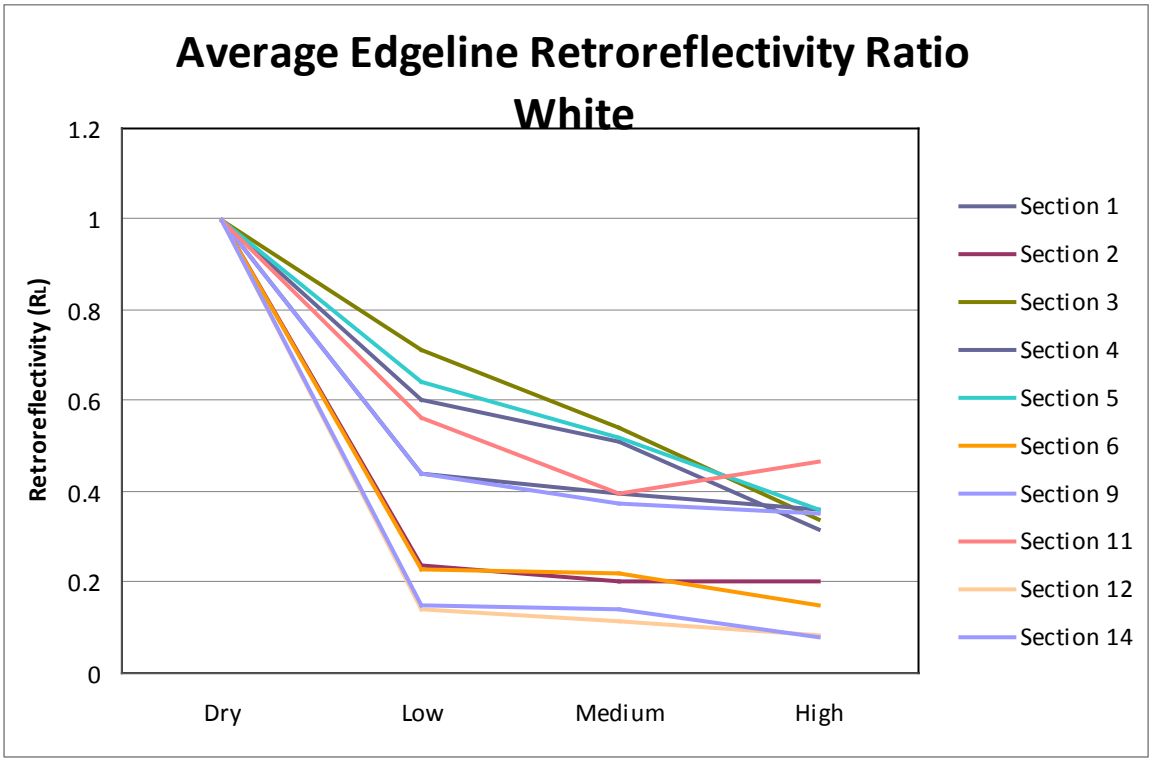

Figure 17. Average White Edgeline Wet Retroreflectivity Ratio from CCD Measurements.

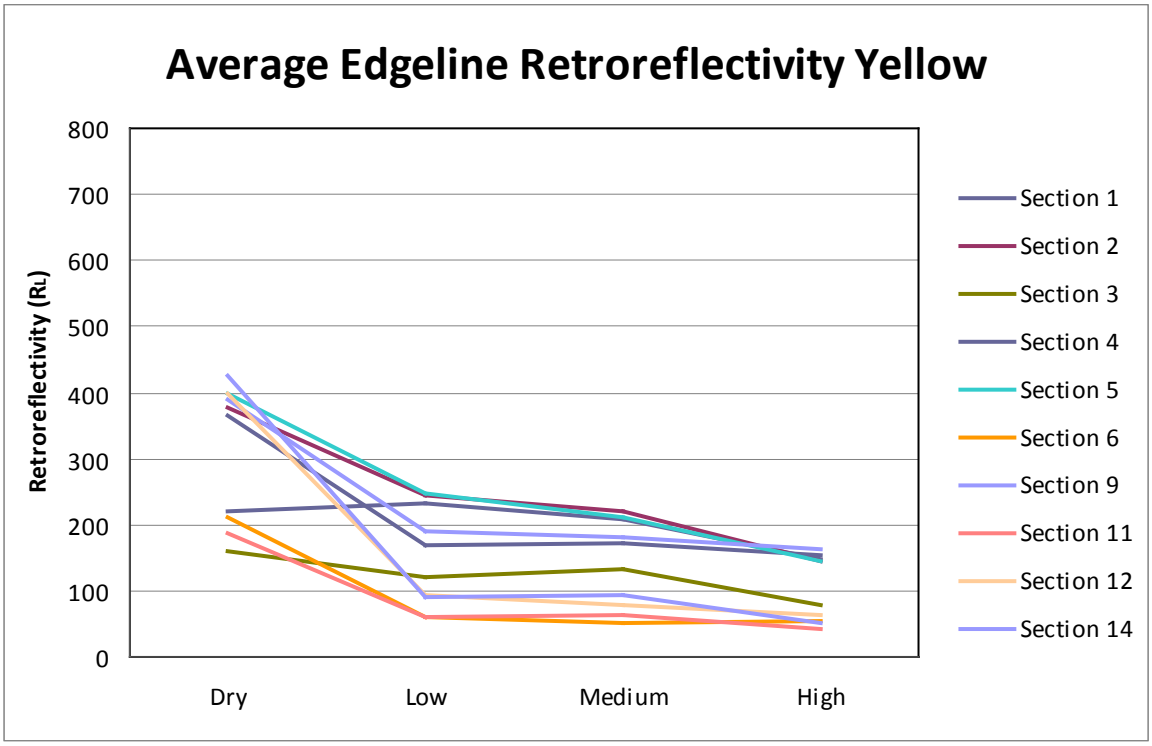

Figure 18. Average Yellow Edgeline Retroreflectivity from CCD Measurements.

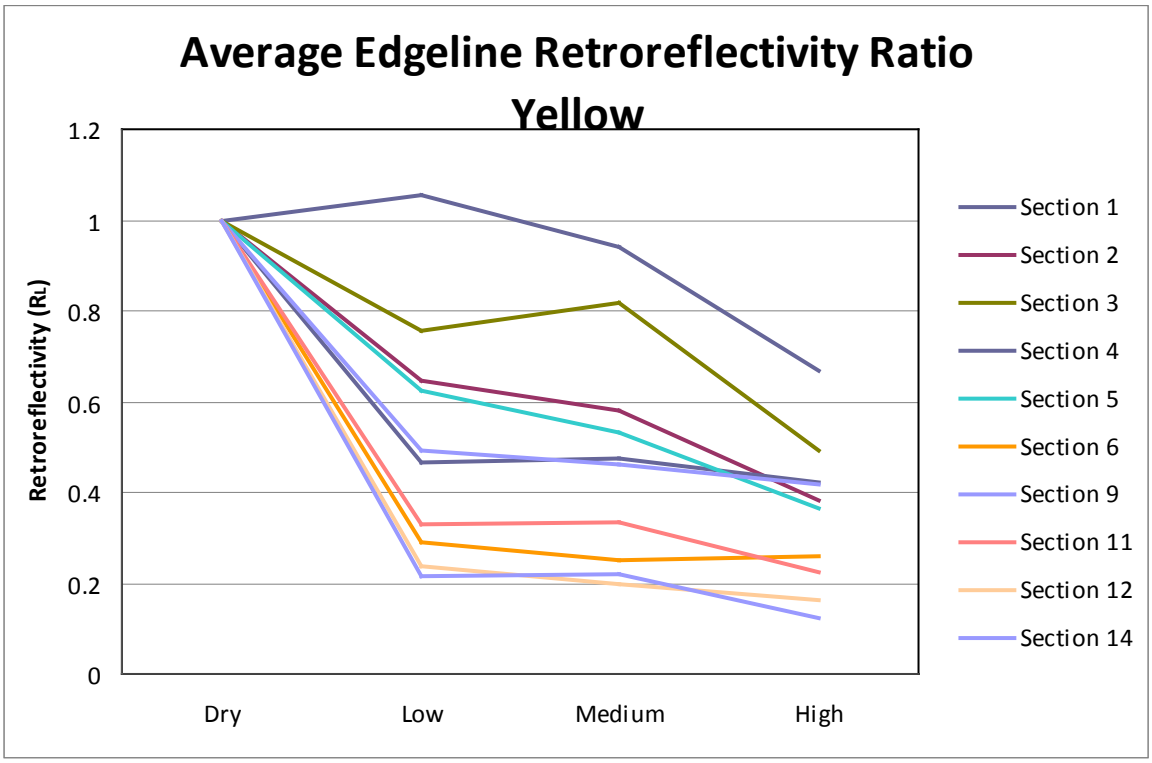

Figure 19. Average Yellow Edgeline Wet Retroreflectivity Ratio from CCD Measurements.

COMPARISON OF MEASURED AND CALCULATED RETROREFLECTIVITY

The previous sections of this chapter describe, among other items, the data from the handheld retroreflectivity measurements and calculated retroreflectivity from the CCD photometer evaluation. This section of the chapter compares the results of these measurements. The intent of this effort is to explore the reliability of handheld retroreflectivity measurements made under dry and various continuous wetting conditions. Appendix G contains a comparison table of all calculated and measured retroreflectivity values for each measurement condition in which similar data were collected (Table 17).

It is important to explain that all but one of the markings evaluated in this effort were specially designed for wet-nighttime performance. The only marking that was not specifically designed for wet-nighttime performance was the standard FDOT application of double drop optics (both optics having 1.5 refractive indices) on non-profiled thermoplastic. Besides this standard FDOT marking (and a double drop thermoplastic marking system employing 1.9 refractive index beads), all of the markings meet the ASTM E2176 criteria of having wet-nighttime performance characteristics. The scope of ASTM E2176 includes the following criteria describing the markings that are intended to be measured under E2176 protocol:

> *This test method has been shown to produce reasonable results for pavement marking systems with optics having an index of refraction greater than 2.0, and structured markings having vertical structures greater than or equal to 3 mm.*[1] *Users should exercise caution when using this test method for pavement marking systems with optics having an index of refraction less than 2.0, or markings having vertical structures less than 3 mm.*

Figure 20 displays a plot of all the data for each marking color. The regression lines indicate that for both the white and yellow markings the coefficient of determination (i.e., R-squared) is approximately 0.9, meaning that there was an overall good correlation between the two measurement techniques. Under ideal conditions the slope of the regression lines would be

[1] The 3 mm minimum vertical structure height is based on a survey of materials evaluated and reported on in: FHWA/VTRC 05-CR3 WET NIGHT VISIBILITY OF PAVEMENT MARKINGS, VTRC (Oct 2004), FHWA/TX-06/0-5008-1 EVALUATION OF WET-WEATHER PAVEMENT MARKINGS: FIRST YEAR REPORT, TTI (Sept 2005), FHWA/TX-07/0-5008-2 EVALUATION OF WET-WEATHER AND CONTRAST PAVEMENT MARKINGS: FINAL REPORT, TTI (Aug 2007).

1 and pass through the origin. An issue that may have biased the CCD measurements to some degree was that there was no way to prevent light from passing vehicles and on-coming vehicles from being included in the readings. Because of the overall lower performance of markings under continuous wetting conditions, the CCD photometer needed as much as 180 seconds per continuous wetting measurement. Ideally only the light from the standard light source, mounted directly above the marking of interest, would be captured during this time. However, the CCD also captured light from passing vehicles and vehicles traveling in the opposite direction across the median. The bias was stronger for yellow pavement markings because of their closer proximity to the opposite direction traffic.

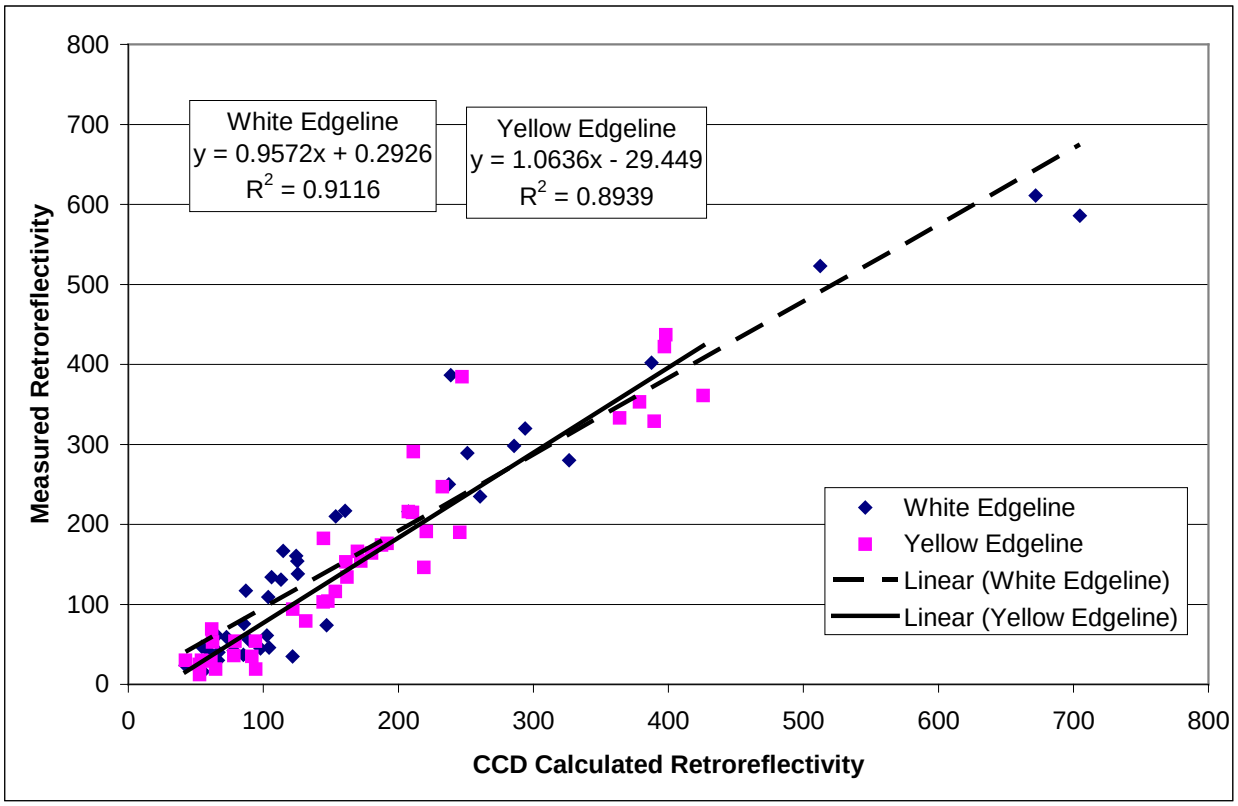

Figure 20. Comparison of Calculated and Measured Retroreflectivity for All Conditions.

Table 1 includes a summary of the Pearson correlation coefficients for each similar measuring technique (the recovery was not performed with the CCD photometer). Table 1 includes correlation coefficients by color and correlation coefficients with the color data combined.

Table 1. Correlation Coefficients for Measured versus Calculated Edgeline Retroreflectivity.

Conditions of Retroreflective Measurements	White Edgeline	Yellow Edgeline	Both Edgelines
Dry	0.940	0.949	0.936
Wetting at 9 iph (ASTM E2176)	0.918	0.903	0.910
Wetting at 2 iph	0.916	0.885	0.884
Wetting at 1 iph	0.879	0.894	0.887

The data from Table 1 indicate there were good correlations between the handheld measurements and the CCD measurements. As expected, the strongest correlations were found when the measurements were taken under dry conditions. This confirms much of the previous research. In addition, the findings show that ASTM E2176 provides strong correlations for pavement markings meeting the ASTM-defined criteria as having wet-nighttime characteristics (optics having an index of refraction greater than 2.0, and structured markings having vertical structures greater than or equal to 3 mm).

The more interesting findings are for the lower wetting rates, which appear to suggest that they produce results that are practically the same as the ASTM E2176 results. However, a closer look at the standard FDOT pavement marking system using double drop 1.5 refractive index beads and the double drop pavement marking system employing high index (1.9) beads (which do not have wet-nighttime performance characteristics as defined in ASTM E2176) shows why there has been controversy over the standard continuous wetting measurement protocol before it was changed to include the limitation for wet-nighttime performance characteristics. Until recently, the ASTM E2176 measurement method was meant to be applied to all markings. However, research results (*6, 7, 8*) and subjective evaluations around the country began to raise concerns about the validity of ASTM E2176 for conventional markings (i.e., those without specially designed characteristics to allow them to maintain their performance in continuous wetting conditions). Overall the main concern was that when conventional markings were measured under the previous E2176 protocol, the measurement results were very low and not always indicative of visibility study results and subjective nighttime evaluations (i.e., conventional markings with very low measured retroreflectivity under the continuous

wetting protocols outlined in ASTM E2176 had similar or even longer detection distances than some markings with higher measured retroreflectivity).

As mentioned previously, the only markings that do not meet the ASTM-defined criteria as having wet-nighttime characteristics were the standard FDOT application of double drop optics (both optics having 1.5 refractive indices) on non-profiled thermoplastic and the double drop optics (using 1.5 and 1.9 refractive index beads) on non-profiled thermoplastic. Under the old ASTM E2176 wetting rate of 9.3 inches per hour, the handheld measurements for these markings were 16 and 24 mcd/m^2/lux for the white markings and 12 and 19 mcd/m^2/lux for the yellow markings, respectively. These extremely low measurements are basically measurement noise (typical road surfaces produce similar retroreflective measurement results) and thus may not be indicative of the true performance of the marking since it is flooded by the high continuous wetting rate. This has been the primary concern over the use of the ASTM E2176 measurement protocol for all markings, especially conventional markings not specifically designed for wet-nighttime performance. It is this reason why ASTM has narrowed the scope of E2176 so that it is only used for markings having optics with indices of refraction greater than 2.0 and structured markings having vertical structures greater than or equal to 3 mm.

Under the lower rainfall rates the standard FDOT marking measured 45 and 19 mcd/m^2/lux for 2 inches per hour and 46 and 35 mcd/m^2/lux for 1 inch per hour for the white and yellow markings, respectively. The double drop marking system using 1.9 refractive index beads measured 41 and 36 mcd/m^2/lux for 2 inches per hour and 59 and 54 mcd/m^2/lux for 1 inch per hour for the white and yellow markings, respectively. These measurements are more representative of the marking in that they indicate that there is some nighttime performance. Subjective nighttime evaluations conducted by FDOT personnel under heavy rain conditions also indicate that while the FDOT standard marking has fairly low wet-nighttime performance, it does indeed have some wet-night performance. Retroreflectivity measurements indicative of noise that would be measured on pavement surfaces without markings are not representative of the markings performance.

It should be noted that in some of the data there were outliers where the data were not strongly correlated. This is probably a function of pavement markings in that they are basically assembled in less than ideal conditions—on the road with traffic in mobile operation. In addition, many of these markings were prototypes and the contractors installing the markings had

limited experience with the marking system details, which was likely to cause some additional variability in the data. Small movements in measurement location between the different methods and the limited number of readings along the markings could also lead to a larger variance in the data.

CHAPTER 4: SUMMARY OF FINDINGS AND RECOMMENDATIONS

Using the latest research approaches and photometric equipment, nighttime pavement marking data were collected in a variety of conditions across a range of pavement marking systems. This chapter summarizes the findings and provides recommendations based on the study findings.

FINDINGS

The data collected with the handheld retroreflectometers indicate that as the continuous wetting rate increases, the retroreflectivity typically decreases. In most situations, the recovery retroreflectivity value is higher than the lowest continuous wetting rate, and the dry retroreflectivity reading is the highest of any condition. The drop in measured retroreflectivity between dry and wet conditions is much larger in some products than it is in others. The yellow markings typically had lower retroreflectivity values than the white markings.

The results from the CCD photometric evaluations provided similar findings to the handheld retroreflectivity data collection. Typically the dry retroreflectivity is the highest and as the continuous wetting rate increases, the retroreflectivity decreases. Some products retroreflectivity ratio comparing wet to dry readings is impacted more than others when measured in continuous wetting conditions.

The color measurements on each marking provided similar results in that the average color was within the required ASTM color boxes. The white edgelines, lane lines, and the yellow edgeline for each section provided adequate daytime and nighttime color readings.

Comparing the handheld continuous wetting measurements to the calculated CCD continuous wetting measurements provided insight into how the handheld measurements correlated to the luminance of the marking. For all measurement conditions, there was a strong linear fit between the handheld and CCD-based retroreflectivity measurements. Closer inspection of the products that did not satisfy the ASTM-defined criteria of having wet-nighttime performance characteristics revealed why ASTM revised E2176 to limit the scope to only markings having optics with indices of refraction greater than 2.0 and structured markings having vertical structures greater than or equal to 3 mm. The lower continuous wetting rates provided as good of a correlation between the handheld and CCD measurements but also provided a more realistic measurement of the retroreflectivity of the standard marking. These

findings were verified by the project director who subjectively rated the markings under a heavy nighttime rainfall event. These findings indicate that the systems and techniques used for data collection were able to produce data that provided representative results.

Variability in measurements can be caused by many factors, and every effort possible should be made to reduce the impact of these factors. Representative locations along a marking should be chosen for measurement. These locations should be free of debris and have a typical cross slope so that the water does not pool on the marking during data collection. Small movements of the wetting device or retroreflectometer may also result in changes in retroreflectivity measurements. These changes are due to the inherent variability of pavement markings in the field. The impact of marking variability can be reduced by taking more measurements at more locations along the marking.

RECOMMENDATIONS

The researchers recommend a measurement protocol for measuring the retroreflective performance of pavement markings systems under continuous wetting conditions that was based on a wetting rate of approximately 2 inches per hour. Appendix B and C provide a complete set of guidelines for the measurement protocol, including detailed drawings and a parts list for the equipment needed to implement the recommended protocol.

CHAPTER 5: REFERENCES

1. ASTM International. Standard Specification for Minimum Retroreflectance of Newly Applied Pavement Marking Using Portable Hand-Operated Instruments. Designation D6359-99. West Conshohocken, Pennsylvania, 1999.
2. ASTM International. Standard Test Method for Measurement of Retroreflective Pavement Marking Materials with CEN-Prescribed Geometry Using a Portable Retroreflectometer. Designation E1710-97. West Conshohocken, Pennsylvania, 1997.
3. ASTM International. Standard Specification for Color of Pavement Marking Materials. Designation D6628-03. West Conshohocken, Pennsylvania, 2003.
4. ASTM International. Standard Test Method for Measuring the Coefficient of Reflected Luminance of Pavement Markings in a Standard Condition of Wetness. Designation E2177-01. West Conshohocken, Pennsylvania, 2001.
5. ASTM International. Standard Test Method for Measuring the Coefficient of Reflected Luminance of Pavement Markings in a Standard Condition of Continuous Wetting. Designation E2176-01. West Conshohocken, Pennsylvania, 2001.
6. Carlson, P.J., J.D. Miles, M.P. Pratt, and A.M. Pike. *Evaluation of Wet-Weather Pavement Markings: First Year Report*. FHWA/TX-06/0-5008-1 Report, Texas Transportation Institute, College Station, Texas, 2005.
7. Carlson, P.J., J.D. Miles, A.M. Pike, and E.S. Park. *Evaluation of Wet-Weather and Contrast Pavement Marking Applications: Final Report*. FHWA/TX-07/0-5008-2, Texas Transportation Institute, College Station, Texas, 2007.
8. Gibbons, R.B., J.M. Hankey, and I. Pashaj. Final Contract Report: Wet Night Visibility of Pavement Markings. VTRC 05-CR3, Virginia Transportation Research Council, 2004.

APPENDIX A: TRANSMISSIVITY ASSESSMENT

EXECUTIVE SUMMARY

Retroreflectivity measurements of pavement markings are typically made through continuous wetting of the marking or in the recovery period just following the wetting. However, this does not accurately represent the visibility of the marking to a driver in a vehicle. Light from vehicle headlamps as well as light reflected from the pavement marking itself are actively attenuated in the rainy atmosphere, and there is a need for a correction to the existing retroreflectivity measurement.

Through controlled experiments on both the Virginia Tech Transportation Institute and the Texas Transportation Institute test tracks, the correction factor to retroreflectivity measurements was addressed. The attenuation of light energy through a simulated rainy atmosphere was investigated and incorporated into the calculation of the transmissivity of light in such conditions. This transmissivity, or amount of light transmitted through the atmosphere, was used in a model to predict certain levels of light. Specifically through measurements of illuminance, luminance, known distances of targets, and rain rates, predictions of light energy loss are made. These predictions can then be applied as a correction to existing retroreflectivity measurements in order to increase accuracy.

Observations into the behavior of light in different rain scenarios are made. Specifically, this addresses the redirection of light through a rainy atmosphere, which can result in an increased object illuminance. The issue of specular reflection off wet pavement is also addressed through the introduction of an equipped baffle for illuminance measurements.

Suggestions for further research are made involving the application of the prediction model to scenarios involving overhead lighting, as well as considerations into the density of the rainy atmosphere for the collection of data. Specifically, this pertains to results from larger water droplets as compared to a finer mist of simulated rain.

INTRODUCTION

The current methods for the evaluation of pavement markings in wet conditions do not account for the impact of the transmissivity of the light through a rainy atmosphere. The retroreflectivity measurements are either made in a continuous wetting condition where the

marking is being sprayed with water or in recovery mode after the wetting has stopped. Neither measurement method represents the actual pavement marking visibility. In a driving scenario, the driver observes the marking through the rain and both the light from the headlamps that illuminates the marking and the light from the marking itself are attenuated by the raindrops.

This experiment is the development of a method of accounting for the transmissivity of the rain-filled atmosphere so that a correction can be applied to the pavement marking retroreflectivity measurement method.

In order to develop the transmissivity of the light through a rain environment, the light reaching the surface of an object (illuminance) and the light being reflected back to the driver/observer (luminance) must be taken into account. The ratio of illuminance of a pavement marking or target in the rain to the illuminance of the same object in a clear condition brings about the attenuation (loss or re-direction) of the light in that atmosphere.

The attenuation may be derived from this formula:

$$Attenuation = \frac{E_R}{E_C}$$

Equation 1

Where:
E_R = illuminance in the rain
E_C = illuminance in the clear condition

Similarly, the luminance-based attenuation may be derived from:

$$Attenuation = \frac{L_R}{L_C}$$

Equation 2

Where:
L_R = luminance in the rain
L_C = luminance in the clear condition

The illuminance-based atmospheric transmissivity (T) is a measurement of the amount of light that is transmitted through some known distance of atmosphere. It is derived from:

$$T = \left(\frac{E_R}{E_C}\right)^{\frac{1}{d}}$$

Equation 3

Where:
d = the distance the light energy must travel in meters

Through this study, the effort is to obtain the atmospheric transmissivity T-value that may then be applied to situations outside this experimental environment. In such cases, with a known T (e.g., illuminance in clear condition, distance light energy has traveled through a rainy environment and rain rate), the level of light that has been lost or redirected due to the rain may then be determined. This unknown rain illuminance may then be expressed as:

$$E_R = E_C * T^d$$

Equation 4

Similarly, the unknown rain luminance may be expressed as:

$$L_R = L_C * T^d$$

Equation 5

These calculations will then be used as prediction models and compared to the measured illuminance and luminance from this study. From this point, a correction factor can be applied to current measures of retroreflectivity of pavement markings.

Research Objectives

Objectives are to collect both illuminance and luminance data in order to determine the level of attenuation of light through the rain atmosphere. Based on the levels of light through the atmosphere, the effort is to make a prediction of the illuminance or luminance of a target and determine the accuracy of such a prediction. Future predictions can then be made based on known clear condition values, distances, and rate of rainfall. This understanding will lead to a more accurate concept of the retroreflectivity of pavement markings.

METHODOLOGY

Design

Virginia Tech Transportation Institute (VTTI) and the Texas Transportation Institute (TTI) each conducted controlled field experiments on their respective test tracks. Independent variables manipulated were presence and rates of rain, distances to targets being measured, and presence of a baffle to decrease specular reflection. Dependent variables measured were the illuminance and luminance of targets. The table below displays the conditions for the VTTI portion of the study (Table 2).

Table 2. VTTI Experimental Conditions.

Variable	Levels
Baffle	With baffle, Without baffle
Rain condition	Clear, Rain flowing, Recovery (wet road, no rain falling)
Location and Rate of Rain	Tower-side ("right") 0.66 iph, Center 1.37 iph, Non-tower side ("left") 0.88 iph
Data Collection Distances (m)	5,15,25,35,45,55,65,75,85

Table 3 displays the specific conditions for the TTI portion of the study.

Table 3. TTI Experimental Conditions.

Variable	Levels
Rain condition	Clear, Rain flowing, Recovery (wet road, no rain falling)
Rain rate	Low (0.28 iph), Medium (0.5 iph), High (0.8 iph)
Data Collection Distances (m)	30,50,70,90

Equipment

VTTI

Measurements of illuminance were made using a T-10 series Minolta illuminance meter and luminance was measured using a Radiant Imaging ProMetric Photometer. The environment for the study was the Virginia Smart Road. The Virginia Smart Road is a 2.2-mile long controlled-access facility. It includes an intersection with functioning traffic lights and a 3/4-mile test bed equipped with custom weather-making towers and overhead lighting. The weather towers are capable of creating rain, snow and fog, and each can be adjusted to desired levels.

In order to decrease the amount of specular reflection from wet pavement, a baffle was designed to fit over the illuminance meter head. The specular reflection phenomenon is displayed below (Figure 21).

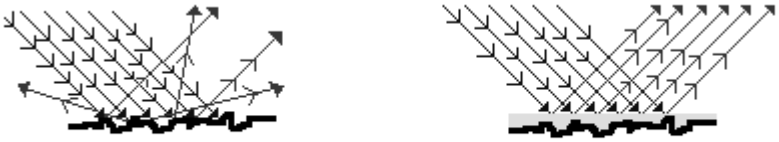

Figure 21. Specular Reflection Effect.

The incoming light approaching the rough, dry surface (Figure 21, left) will reflect in multiple directions and angles depending on its angle upon reaching the ground surface. The depiction on the right portrays light approaching a wet surface. As water has filled the rough terrain, a greater percentage of approaching light is reflected at a concentrated level toward an illuminance meter or vehicle operator. The baffle (Figure 22) was designed to minimize this effect on data being measured.

Figure 22. Baffle with Illuminance Head Mounted.

This baffle was a 12-in. long tube designed to allow only direct light to be received by an illuminance meter head installed at one end of the tube. The baffle was mounted approximately 5 feet above the road surface on a tripod. Targets (10 1/4 x 7 1/4 in.**)** were employed for measurements of illuminance and luminance (see Figure 23).

Figure 23. Example of VTTI Target.

The light source was a single halogen Ford Explorer headlamp mounted on a mobile cart positioned 5 meters outside of the rain-test area of targets. For example, while a target was 20 meters from the light source, the distance of the rain-covered area was really 15 meters. This cart held the photometer and allowed lateral movement across two lanes of the test area. Rain gauges were used throughout the testing area in order to determine the rate of rain falling.

TTI

Illuminance was measured using a T-10 Minolta illuminance meter. The same Radiant Imaging ProMetric Photometer used in the VTTI study was also employed for the TTI study. The environment for the study was the TTI rain tunnel system. Approximately 1600 feet long, the rain tunnel consists of 250 risers, with nozzles extending 10 feet above the road surface. Targets (12 x 12 in.) were diffuse reflectors and were employed for measurements of illuminance and luminance. The light source used was a set of halogen low beams on a Ford Taurus. This vehicle was positioned outside of the rain-test area of targets.

Procedure

VTTI

Measurements were taken over the course of a 2-hour period after sunset. Targets were set up on the Smart Road's rain tower portion of the road, every 5 meters up to 45 meters from the light source. Targets were also added at 60 and 80 meters from the light source. Figure 24 provides a diagram of the VTTI setup.

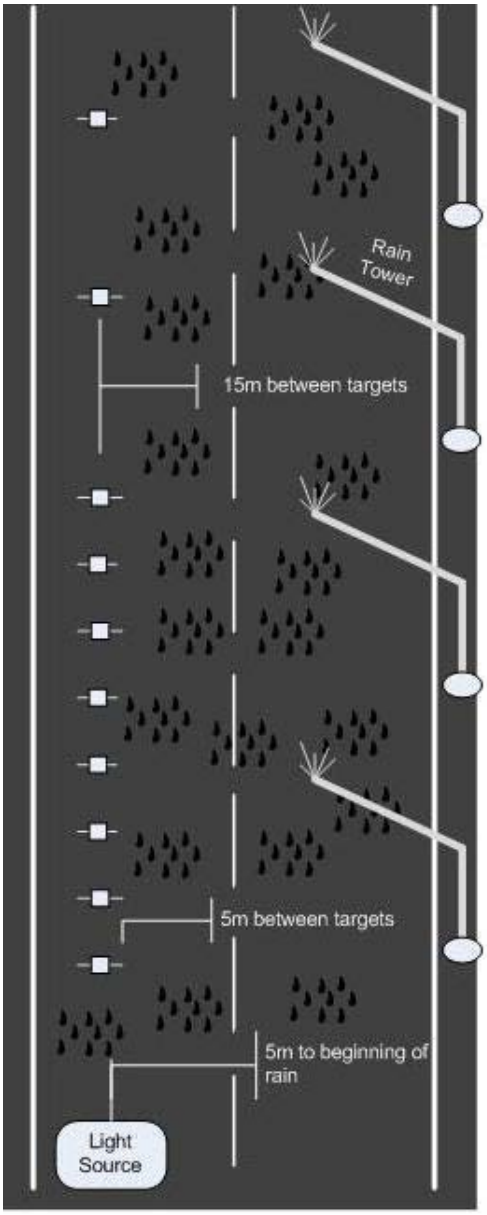

Figure 24. VTTI Setup of Targets in Rain Portion of Road.

Measurements were taken for dry conditions, rain conditions, and recovery/wet road conditions. Measurements were taken with the illuminance meter at all distances designated by targets, as well as with a baffle surrounding the illuminance meter receptor head. These additional measurements were taken at 5-meter increments from 10 to 90 meters from the light source. The baffle was mounted on a tripod approximately 5 feet above ground level. When measurements were completed for a row of targets on the non-tower side of the test area, targets were moved laterally across the road for another set of measurements up to 90 meters from the light source. Targets continued to be moved in this fashion, across the center of the road, and ending at the tower side of the test area. Figure 25 provides and example of one of the experimental layouts of the targets on the test area.

Figure 25. VTTI Target Layout.

Luminance measurements were collected through the use of the photometer mounted with the light source. Images captured by this photometer were analyzed following the data collection. Luminance data reported were an average of values extracted from the targets, excluding portions of the target with high glare due to the light source. Targets of interest from

this luminance analysis were located 10 to 45 meters from the source. Rain from the towers was falling at an average rate of 0.66 iph for the tower side of the road ("right"), 1.37 iph for the center, and 0.88 iph for the non-tower side ("left"). The rates reported are averages of numerous rain gauges distributed along the respective portions of the test area.

TTI

TTI's test area consisted of targets placed at 30, 50, 70, and 90 meters away from the light source. Targets were standing vertically on the road surface perpendicular to the light source. Targets were slightly offset from each other to avoid shadows on target surfaces. The photometer was positioned inside the vehicle outside of the rain-test area. Illuminance data were collected using illuminance meters at target locations. Luminance data were collected through images captured by the photometer inside of the vehicle. Images were analyzed following data collection. Luminance results were an average of values from a constant coordinate location in the image over the course of multiple images captured. The rain system provided three different rain rates of High (0.8 iph), Medium (0.5 iph), and Low (0.28 iph). Measurements were taken for dry conditions, rain conditions, and recovery/wet road conditions.

Data Analysis

Data include the percentage of light transmitted by comparing the clear to rainy conditions by institute (VTTI and TTI). The level of attenuation taking place through the rainy atmosphere would then be implemented to calculate the atmospheric transmissivity (T). Based on an average T-value for each level of rain, a prediction of the illuminance-based attenuation was made. A correlation of the predicted illuminance to actual illuminance was then made. The results section goes through this process for the illuminance measurements, followed by the luminance measurements.

Following the calculations of this prediction model, there is a comparison of data measured through the use of the baffle (the VTTI study) to data obtained without a baffle (part of VTTI and TTI study).

RESULTS

Illuminance

Figure 26 displays the ratio of light transmitted through the rain-test area during active rain and clear conditions for the portion of the study conducted at VTTI. Data are separated by the levels of falling rain measured, as well as the stationary target measurements and use of the baffle around the illuminance meter.

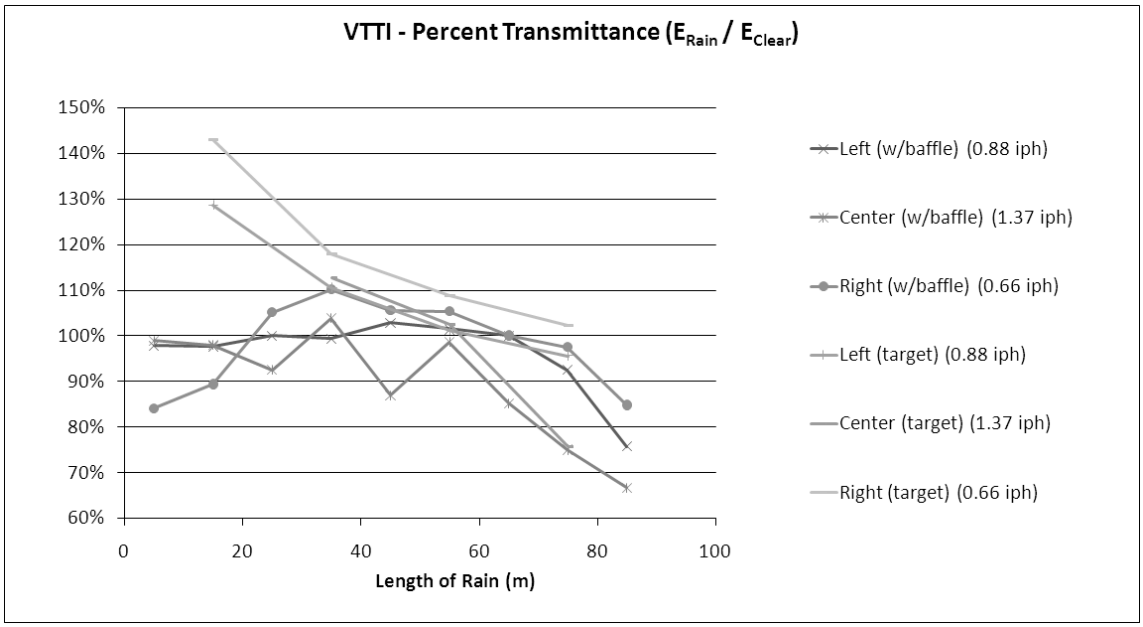

Figure 26. Percentage of Light Energy Transmitted through Rain-Test Area – VTTI.

The data are consistent with the assumption that the level of light transmitted through the atmosphere decreases with increased distance from the light source. What is interesting to note are the relatively high percentages (above 100 percent) of light being transmitted through the rainy atmosphere. Possible explanations for this would be the actual redirection of light in the rainy atmosphere or the internal reflection of light inside the baffle to the illuminance meter receptor head. Concerning the redirection of light, there is specifically the concept of forward scatter of light (see Figure 27).

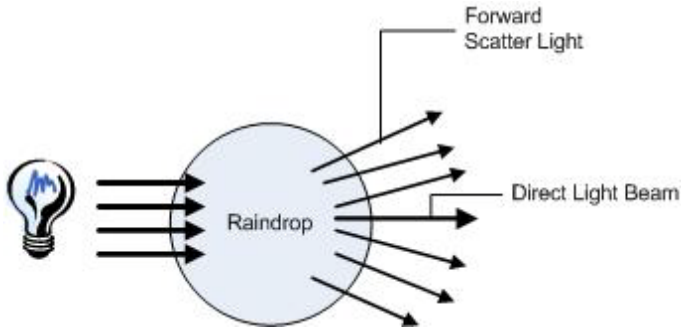

Figure 27. Forward Scatter of Light.

When the light from a source comes in contact with a raindrop in the atmosphere, the majority of light travels directly through as if the raindrop were absent. However, there is also a scattering and redirection of light continuing forward through the raindrop. This scattering, although of less intensity than the direct beam, would explain the increased illuminance readings. This would include light that would have been undetected by the illuminance meter if the rain were not present.

Consistent with expectations, the highest rain rate (Center) resulted in a lower percentage of light transmitted further from the light source. Similarly, the lowest rain rate (Right) resulted in the highest percentage of light transmitted over the course of the distance. The data collected through the baffle indicate slight increases in percentage of transmission, followed by steady decreases after about 60 meters of rainy atmosphere. In contrast, target data indicate a steady decrease in transmission. A possible explanation for this would be the location of the baffle as compared to the targets. Targets were positioned on ground level while the baffle's positioning was elevated above the ground level approximately 5 feet. The distribution of light's intensity from the headlamp would explain the difference between a measurement at ground level and one at 5 feet above ground level. Figure 28 displays the results of the TTI portion of illuminance measurements and percentage of light transmitted.

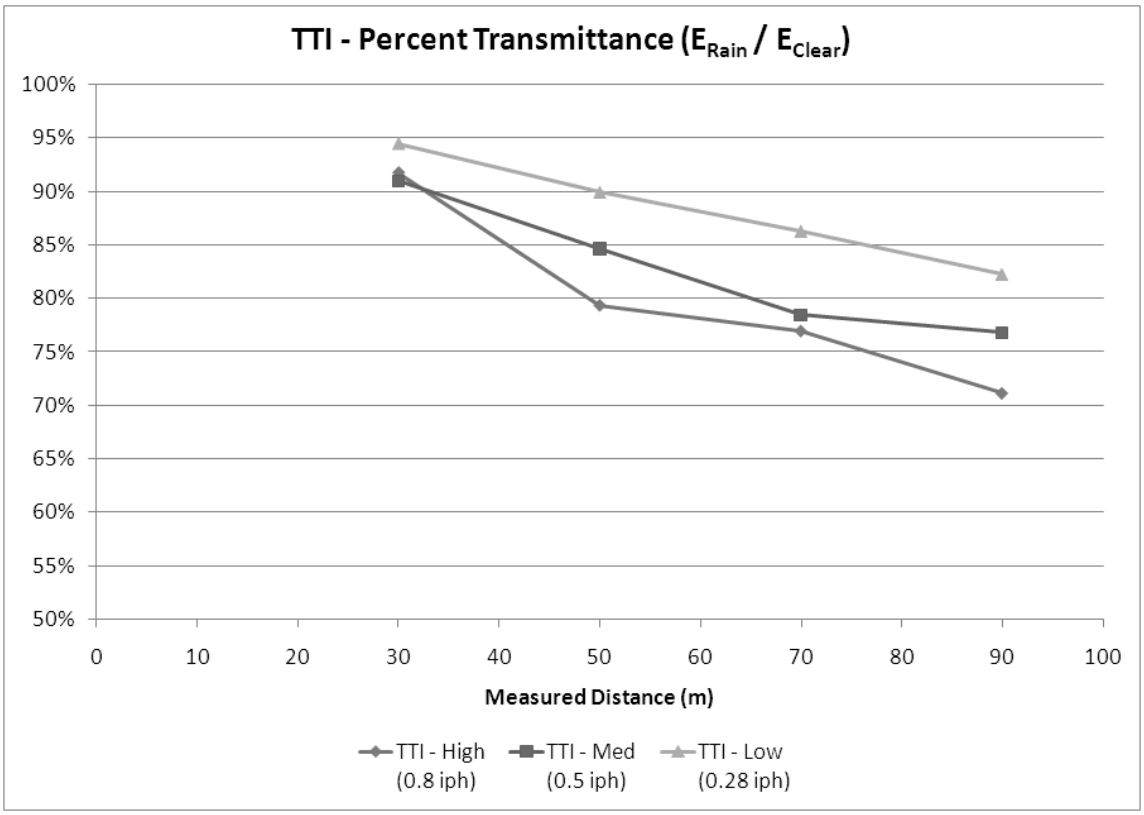

Figure 28. Percentage of Light Energy Transmitted through Rain-Test Area - TTI Study.

Similar to VTTI, these results indicate the decrease in light transmitted over distance. Consistent with expectations, the lowest percentage of light transmitted occurred at the highest rain rate. The variability in the relationship between the medium and high rain setting may be a result of the uncertainty in the measurements. For both VTTI and TTI, the methods of making continuous rain rely on spraying water into the atmosphere. The flow of these drops may be influenced by the ambient atmosphere. This may lead to a high level of measurement uncertainty as the measurement cycle can be time consuming. As the impact of the atmosphere on the rain is influenced by droplet size, the measurement uncertainty may be higher in one location or rain rate than the other. Further investigation into the impact of the rain droplet consistency on the measurement uncertainty should be conducted.

Figure 29 and Figure 30 are based on the calculation of the transmitted light energy through the rain-test area (Equation 3). This calculation is a ratio taking into account the distance the light had actually traveled in both clear and rainy scenarios.

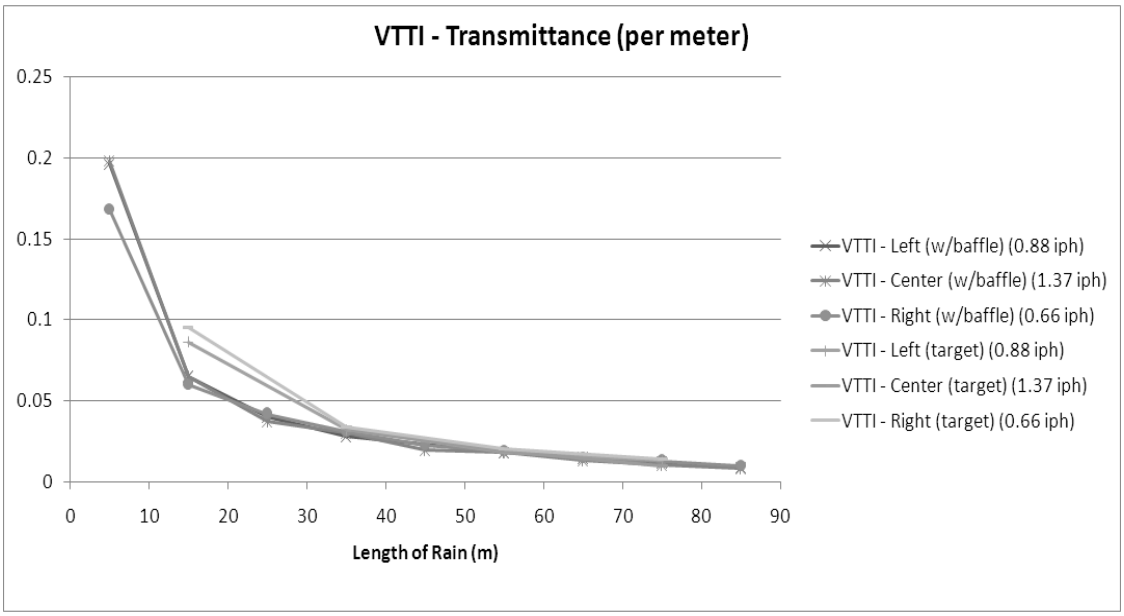

Figure 29. Transmittance of Light per Meter through Rain-Test Area - VTTI Study.

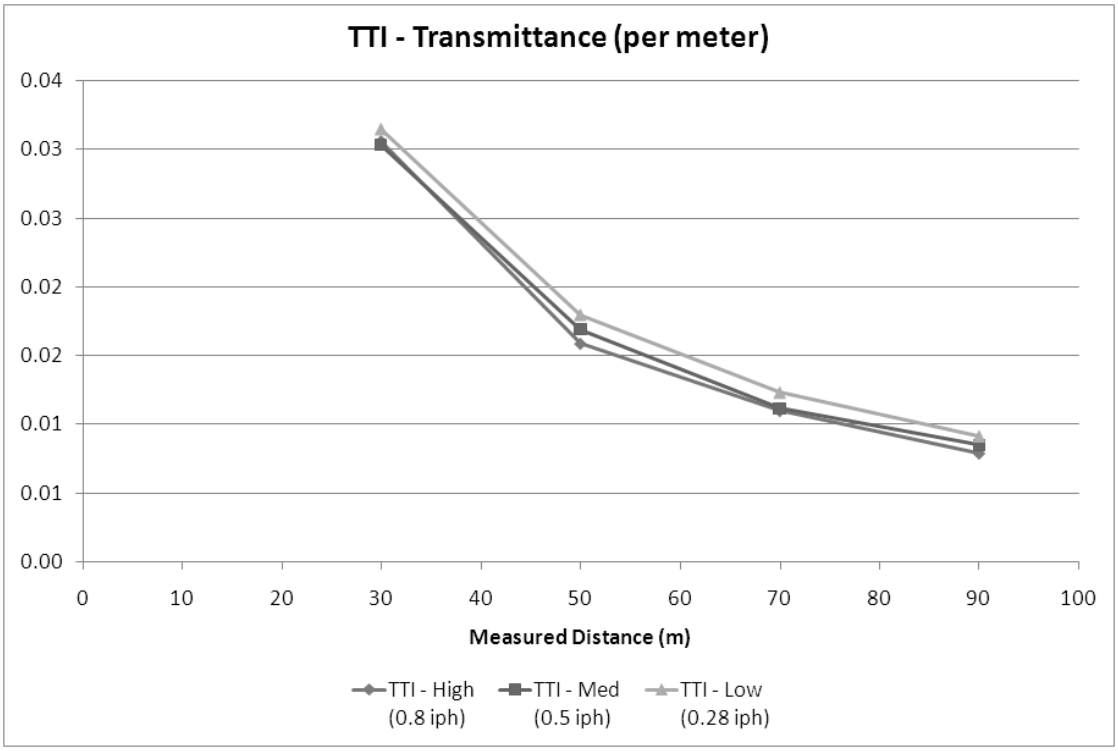

Figure 30. Transmittance of Light per Meter through Rain-Test Area - TTI Study.

The VTTI data indicate a minute difference between the Center and Left measurement locations in terms of transmittance of light per meter. All other measured data of transmittance of light are consistent with expectations of increased distance. It is interesting to note as a comparison between institutes that VTTI results beyond 25 meters appear to be similar to TTI

results at comparable distances. These T-values may then be incorporated to predict the illuminance of the target based on a known rain rate, clear illuminance, and distance to target.

With the collected data, a prediction of illuminance can then be made using Equation 4. Figure 31 and Figure 32 display the relationship of such predictions as well as the correlation of the prediction to the actual illuminance measured.

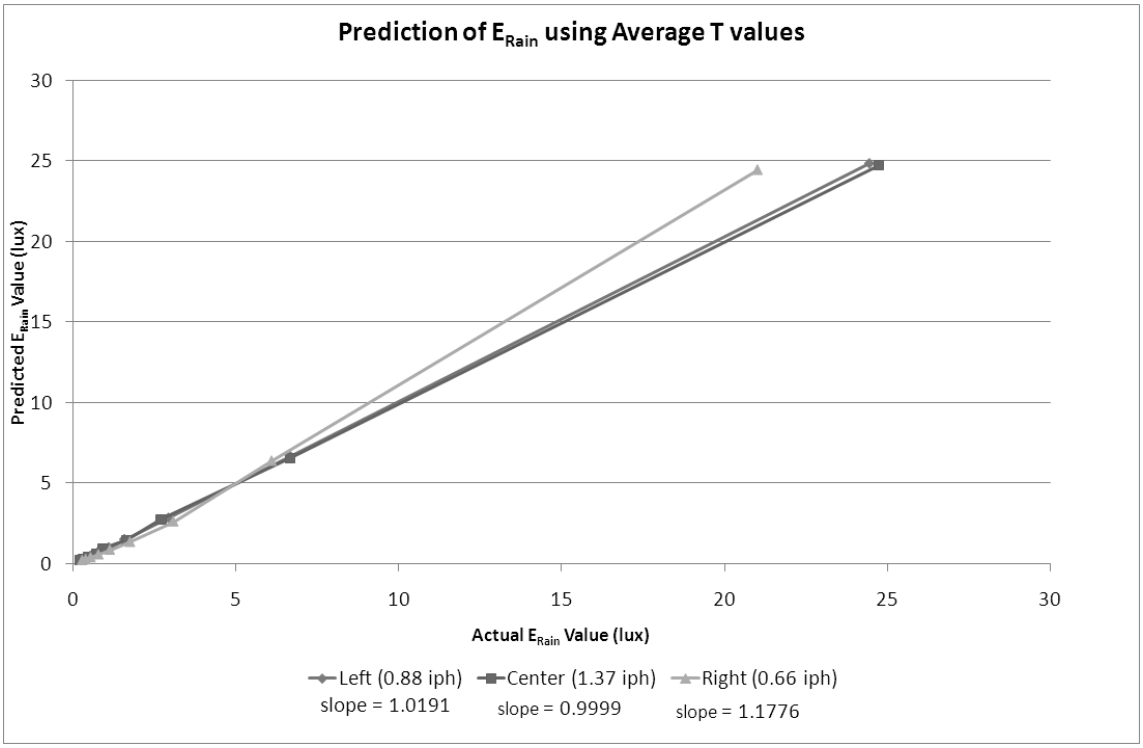

Figure 31. Prediction of Illuminance Based on Atmospheric Transmissivity - VTTI Study.

The slopes of the lines in Figure 31 indicate the correlation of the relationship of predicted illuminance to actual illuminance. With a slope equal to 1, this would indicate a direct 1-to-1 relationship of the prediction to actual measurements. As indicated in the results, the slopes are approximately at this level of correlation. However, with such a limited sample size of nine distances, it is difficult to put much weight on the statistical significance of such predictions. Table 4 displays the data collected in order to provide a clear breakdown of the results.

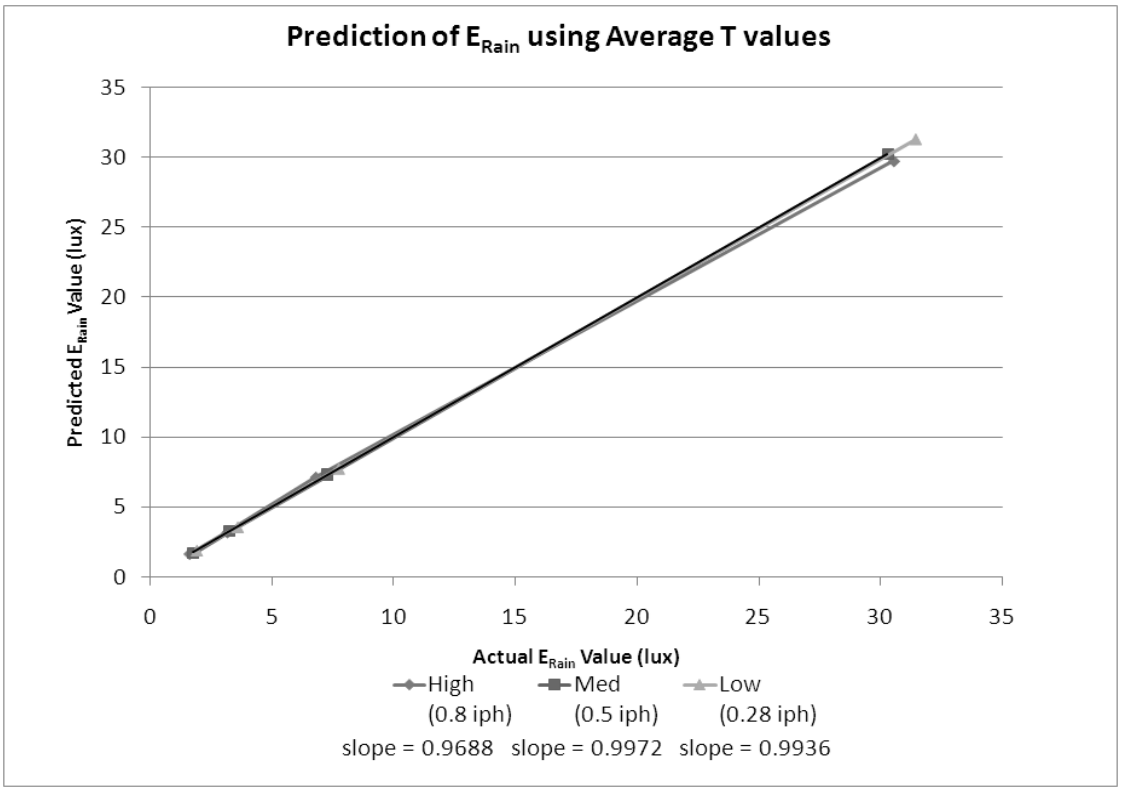

Figure 32. Prediction of Illuminance Based on Atmospheric Transmissivity - TTI Study.

Table 4. VTTI - Prediction of Illuminance.

	Actual (lux)	**Predicted (lux)**	**Actual (lux)**	**Predicted (lux)**	**Actual (lux)**	**Predicted (lux)**
Length of Rain (m)	VTTI - Left (w/baffle)	(0.88 iph)	VTTI - Center (w/baffle)	(1.37 iph)	VTTI - Right (w/baffle)	(0.66 iph)
5	24.45	24.88	24.73	24.73	21.03	24.50
15	6.66	6.71	6.68	6.60	6.10	6.41
25	2.93	2.85	2.71	2.77	3.08	2.64
35	1.58	1.53	1.65	1.47	1.75	1.38
45	1.10	1.02	0.93	0.97	1.13	0.89
55	0.75	0.70	0.73	0.65	0.78	0.59
65	0.54	0.50	0.46	0.47	0.54	0.41
75	0.37	0.37	0.30	0.34	0.39	0.29
85	0.25	0.30	0.22	0.27	0.28	0.23

The majority of the predictions (approx. 66 percent) were within 15 percent of the actual measured illuminance. The predictions that were outside of this 15 percent range existed primarily in the low intensity illuminances where the margin of error is relatively small compared to higher intensity illuminance.

Similar to VTTI's findings, the TTI-conducted study resulted in a strong ability to predict rainy atmosphere illuminance, with a correlation close to 1. Table 5 displays the specific data collected in a comparison to the model-based prediction. All predictions were within 10 percent of the actual measured illuminance.

Table 5. TTI - Prediction of Illuminance.

	Actual (lux)	**Predicted (lux)**	**Actual (lux)**	**Predicted (lux)**	**Actual (lux)**	**Predicted (lux)**
Distance to Light (m)	High (0.8 iph)		Med (0.5 iph)		Low (0.28 iph)	
30	30.55	29.75	30.30	30.23	31.45	31.28
50	6.83	7.13	7.28	7.32	7.73	7.75
70	3.19	3.19	3.25	3.31	3.58	3.58
90	1.64	1.64	1.77	1.72	1.90	1.91

Luminance

Figure 33 displays the measured luminance of targets through the rain-test areas. The following data are the result of the use of the photometer and analysis of images following the data collection; therefore, there was no use of a baffle for measurements.

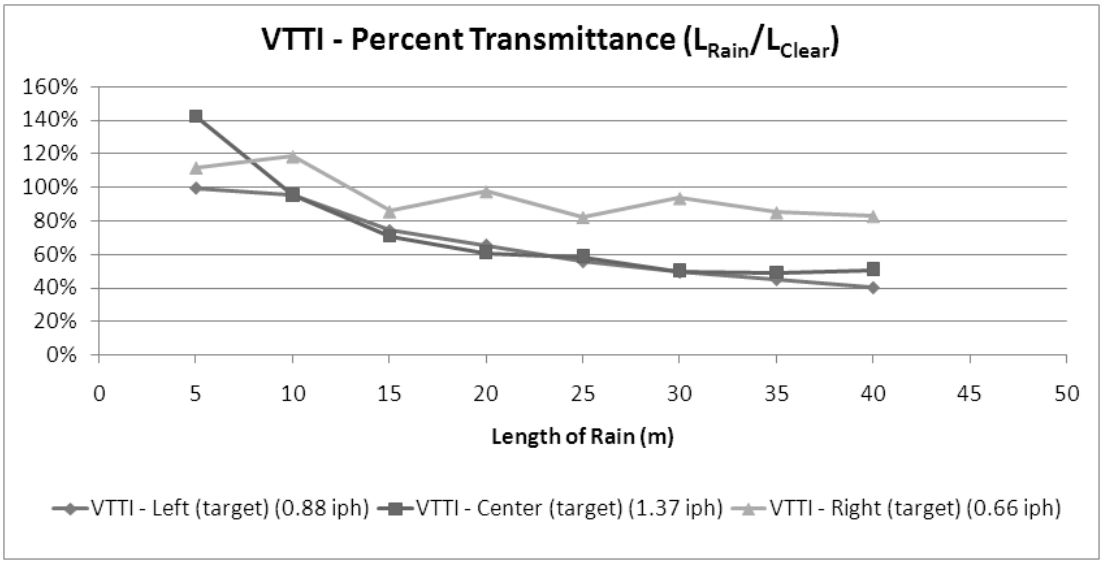

Figure 33. Percentage of Light Energy Transmitted through Rain-Test Area - Luminance Data – VTTI.

The least intense rain rate of 0.66 iph resulted in the greatest percentage of light transmitted through the rainy atmosphere. This is consistent with expectations as well as with illuminance data. Also in similarity to illuminance data, the luminance data exhibit percentages of light transmitted beyond the 100 percent mark. Again, possible explanations for this include the redirection or forward scatter of light discussed earlier. It should be noted that the light being measured in these instances was directed from the source through the rainy atmosphere to the target and then through the atmosphere again to the photometer location near the source. These data then reflect a double-attenuated level of light as well as a greater opportunity for redirection of light within the atmosphere. Figure 34 displays the percentages of transmitted light for the TTI-conducted study.

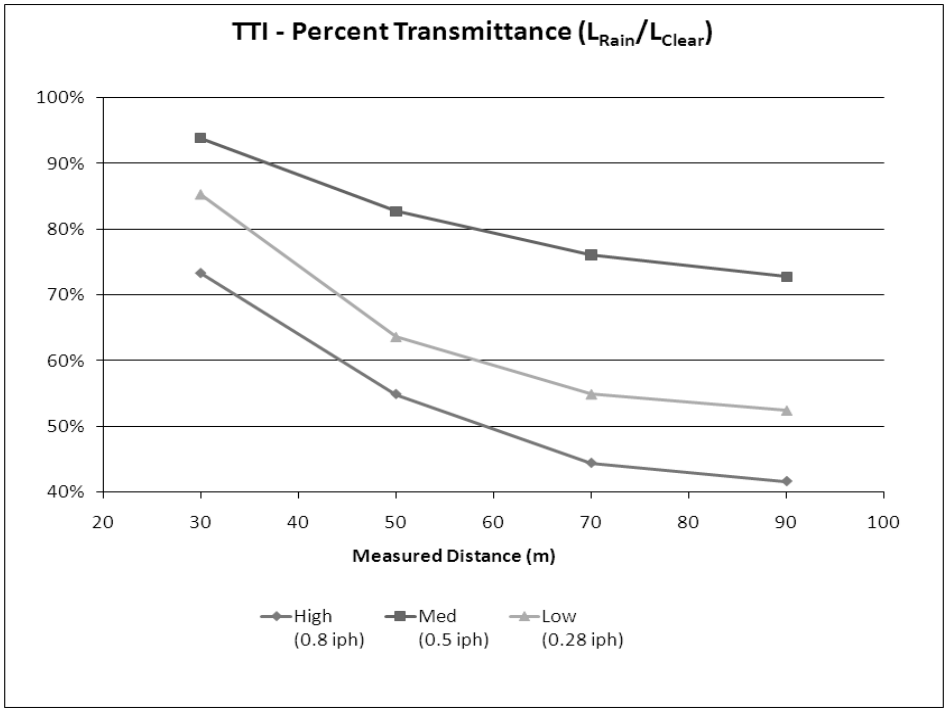

Figure 34. Percentage of Light Energy Transmitted through Rain-Test Area - Luminance Data – TTI.

Contrary to the illuminance results, these luminance results indicate a relatively high percentage of light transmitted through the Medium rain rate of large water droplets as compared to the Low rate delivering a fine mist. With the consistently higher percentage of light at the Medium rate, it would seem that the behavior of light in a fine mist as compared to the larger droplets may prompt further investigation.

With the knowledge of the above attenuation levels of light, the atmospheric transmissivity levels were calculated and are presented in Figure 35 and Figure 36.

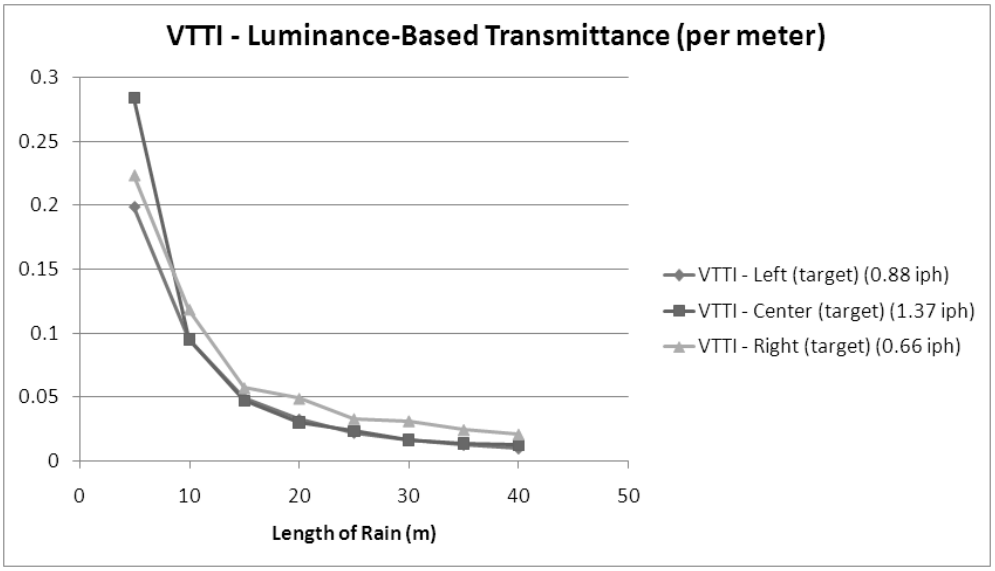

Figure 35. Transmittance of Light per Meter through Rain-Test Area - Luminance Data – VTTI.

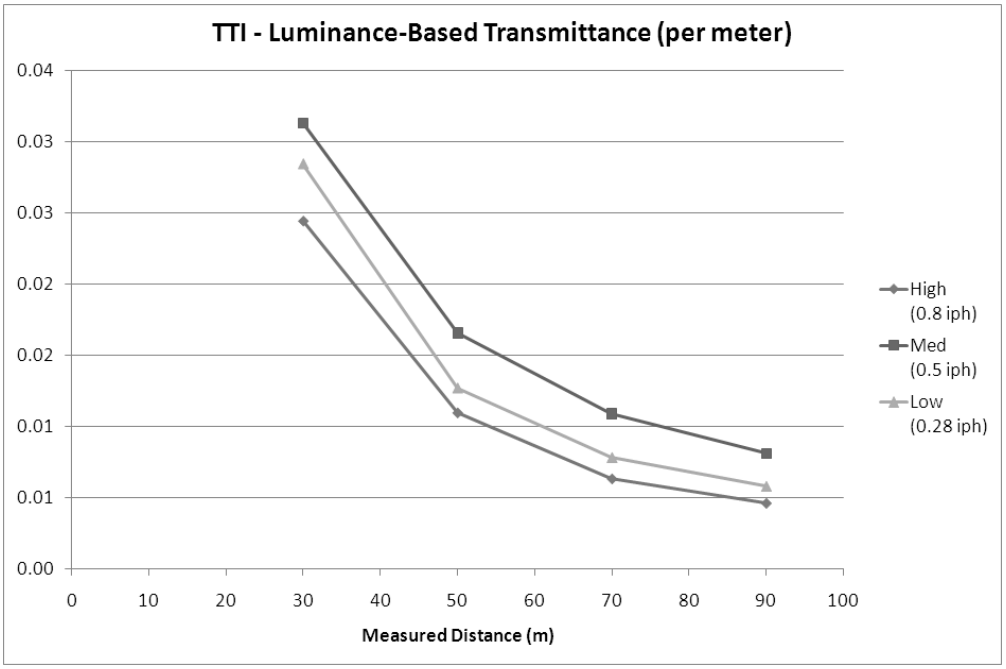

Figure 36. Transmittance of Light per Meter through Rain-Test Area - Luminance Data – TTI.

These luminance-based results seem consistent with expectations based on the results of the percentage of light transmitted. Comparisons between institutes also appear consistent, as

transmittance of light calculated beyond approximately 25 meters again appears similar. Derivation of the prediction model for luminance-based transmissivity is then possible through Equation 5 and the results are presented below (Figure 37).

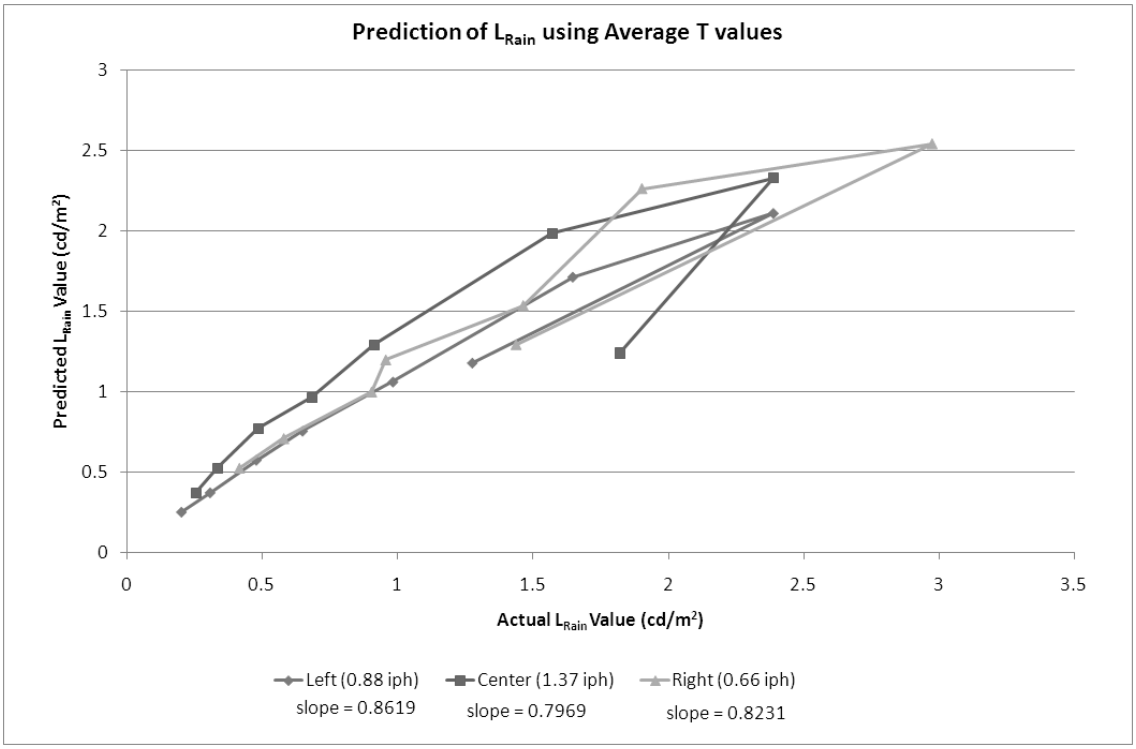

Figure 37. Prediction of Luminance Based on Atmospheric Transmissivity - VTTI Study.

Reasoning for the appearance of a somewhat nonlinear trend is best explained by the distribution of the light from the source. The smallest luminance values above are associated with the furthest distance from the light source. As the distance from targets to the source decreases, there is an expected trend of increasing luminance values. However, the data collected at the closest distance to the light source (10 meters) shows an unexpected decrease in luminance. This is present for each of the three road locations. A possible explanation for this discontinuity is due to its location as being the front-most target. Being the front-most target, this location lacks a target (and its shadow) immediately in front of it. Therefore, it may be assumed that the front-most target is affected by the specular reflection of light more than the locations beyond it.

The correlations of the prediction to the actual luminance measurements are, therefore, not as strong as illuminance results. One explanation for this would be the impact of the data from the front-most target.

Table 6 displays the specific data points collected for the VTTI data.

Table 6. VTTI - Prediction of Luminance.

	Actual (cd/m^2)	Predicted (cd/m^2)	Actual (cd/m^2)	Predicted (cd/m^2)	Actual (cd/m^2)	Predicted (cd/m^2)
Length of Rain (m)	VTTI - Left (0.88 iph)		VTTI - Center (1.37 iph)		VTTI - Right (0.66 iph)	
5	1.28	1.18	1.82	1.24	1.44	1.29
10	2.39	2.11	2.39	2.33	2.97	2.54
15	1.65	1.71	1.57	1.98	1.90	2.26
20	0.99	1.06	0.91	1.29	1.46	1.53
25	0.65	0.76	0.68	0.96	0.96	1.20
30	0.48	0.57	0.49	0.77	0.91	1.00
35	0.31	0.37	0.34	0.52	0.58	0.71
40	0.20	0.25	0.26	0.37	0.42	0.53

Figure 38 displays the results of the luminance prediction based on the TTI-collected data.

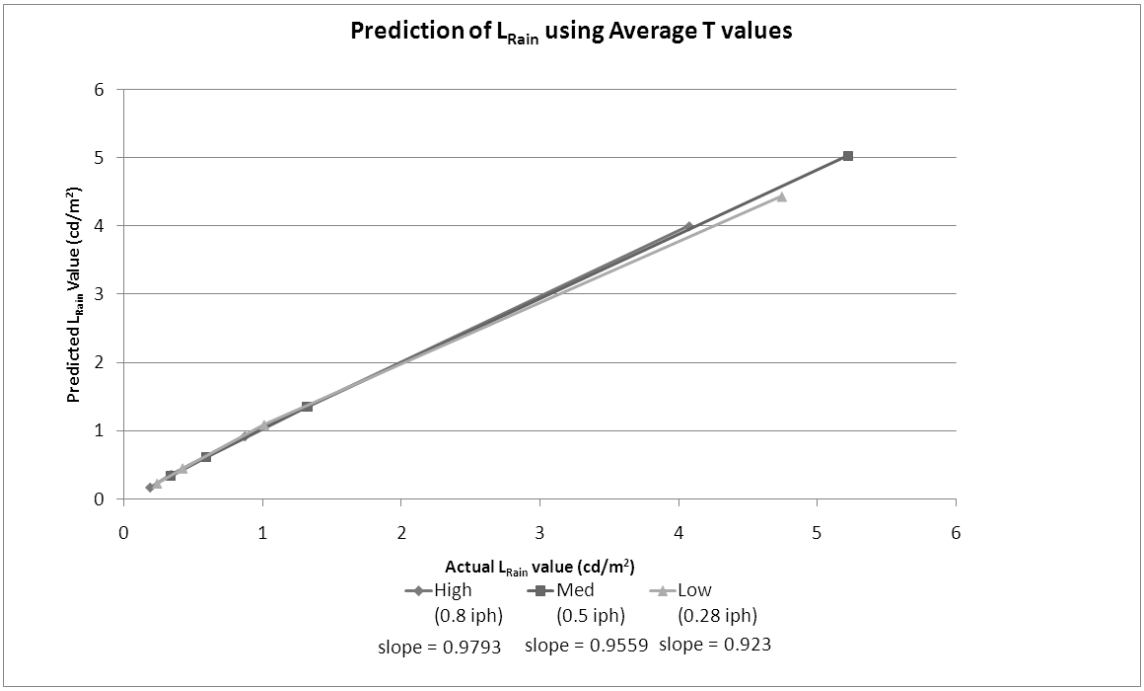

Figure 38. Prediction of Luminance Based on Atmospheric Transmissivity - TTI Study.

Results of this prediction model also show high correlation, close to a 1-to-1 relationship of predicted luminance to actual luminance. All predictions of luminance were within 11 percent of the actual measured luminance. Table 7 displays the specific data points recorded and predicted for the TTI data.

Table 7. TTI - Prediction of Luminance.

	Actual (cd/m^2)	**Predicted (cd/m^2)**	**Actual (cd/m^2)**	**Predicted (cd/m^2)**	**Actual (cd/m^2)**	**Predicted (cd/m^2)**
Distance to Light (m)	High (0.8 iph)		Med (0.5 iph)		Low (0.28 iph)	
30	4.08	4.01	5.22	5.03	4.74	4.44
50	0.87	0.92	1.32	1.35	1.01	1.09
70	0.34	0.36	0.59	0.61	0.42	0.46
90	0.19	0.17	0.34	0.34	0.24	0.23

While prediction strength is high in both the VTTI and TTI test situations, it is interesting to note the characteristic of the maximum values of the specific data collected. In particular, the maximum average luminance collected from a target was approximately 3 cd/m^2 in the VTTI portion and 5 cd/m^2 in the TTI portion. Future research prompts the question of what impact higher luminance values through overhead lighting would have on the prediction strength.

Influence of Baffle

The results of a comparison of the recovery/wet period (no active rain being applied) to the clear condition before simulated rain is introduced are presented below by institute (Figure 39, Figure 40, and Figure 41. The effect of the use of the baffle is presented first. Results indicate that the baffle appears to have been successful at decreasing specular reflection from the road surface, as illuminance measurements are nearly indistinguishable between the completely clear condition and the wet condition after simulated rain has fallen. This becomes more evident as compared to data collected without the use of a baffle in Figure 40.

The results from both VTTI and TTI show slightly higher illuminance measurements from recovery/wet pavement conditions compared to clear/dry conditions. This demonstrates the subtle impact of specular reflection off wet pavement, as well as a reminder of what a driver may experience viewing wet pavement markings following rainfall. This introduces the consideration

of what the reflection of light off pavement markings in an overhead lighting scenario may bring to a driver.

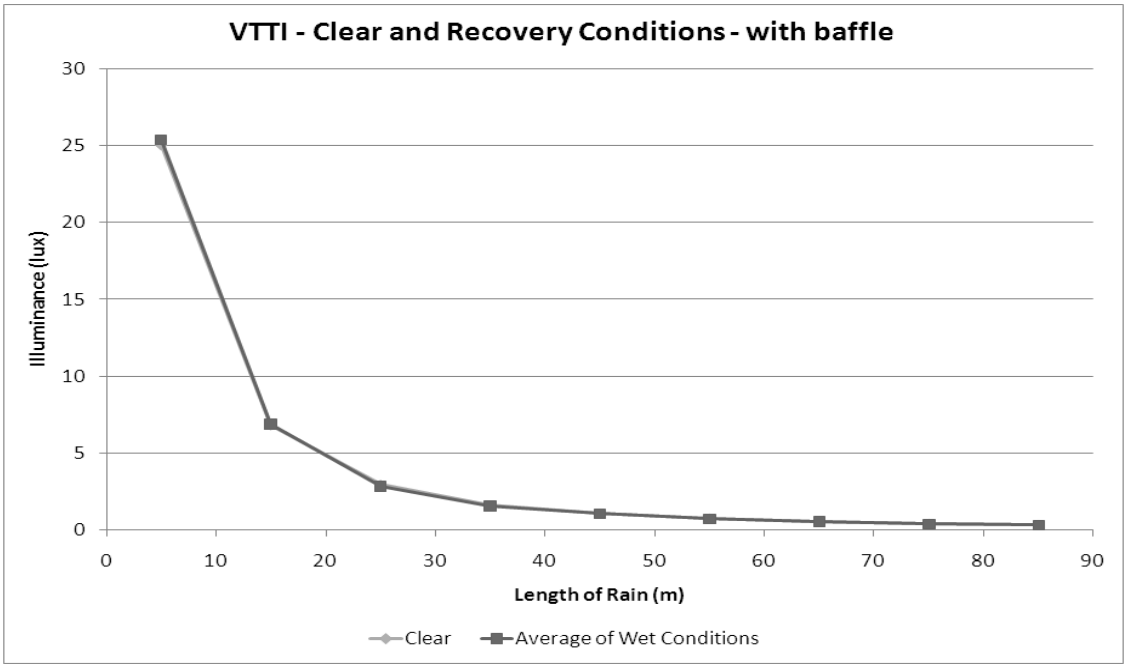

Figure 39. Comparison of Clear Condition to Recovery Period following Rain - VTTI Study.

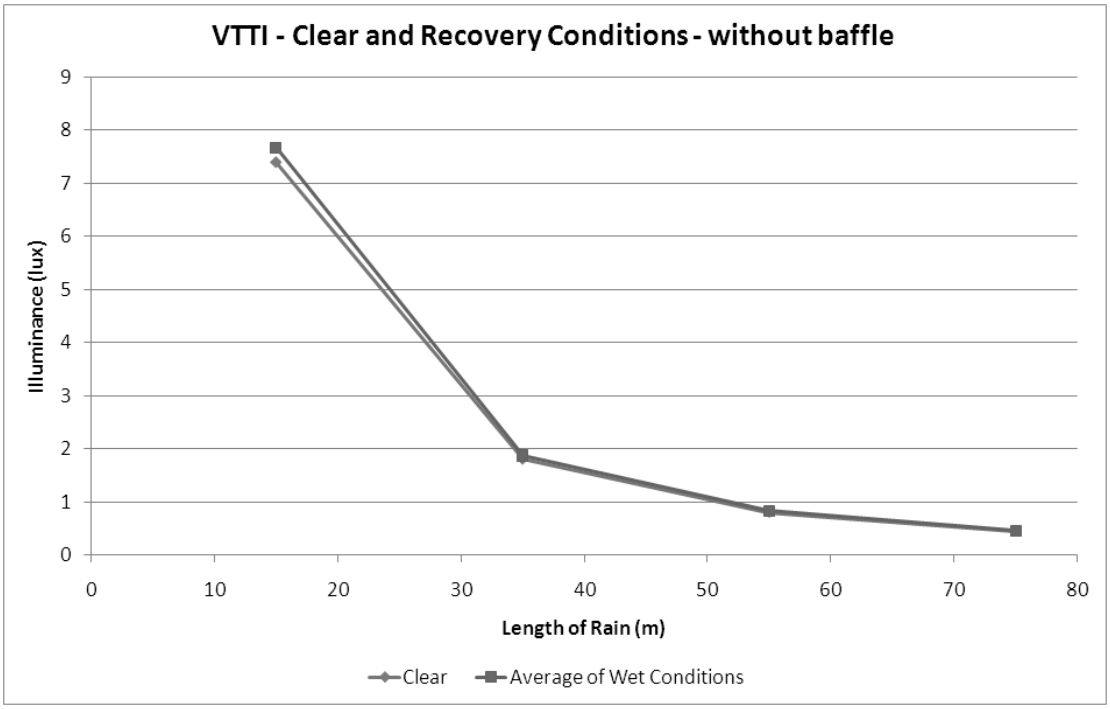

Figure 40. Comparison of Clear Condition to Recovery Period following Rain (without Baffle) - VTTI Study.

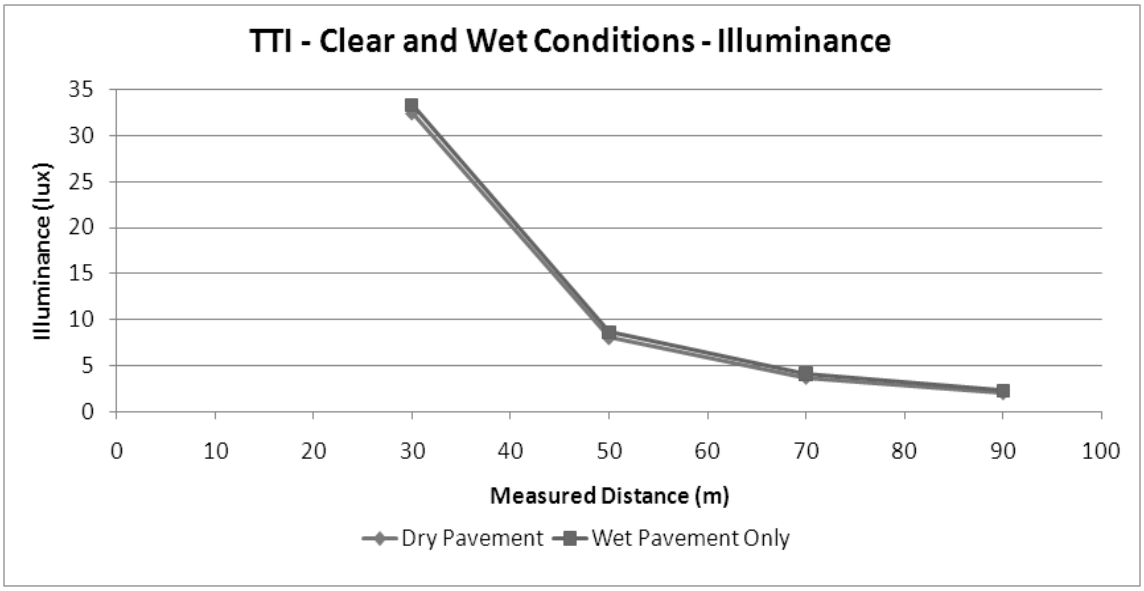

Figure 41. Comparison of Clear Condition to Wet Pavement Condition - TTI Study.

DISCUSSION

Through both illuminance- and luminance-based means, the prediction of attenuation of light through a rainy atmosphere was found to be statistically accurate based on the sample sizes in the VTTI and TTI portions of the study. This prediction was the result of a factor of distance, the illuminance or luminance of an object in the clear atmospheric condition, as well as the derived atmospheric transmissivity for the tested rain rates.

It is also important to note that with the results of the luminance-based data, one must consider the light energy as having traveled both from the source to the target, as well as back again to the measuring photometer. Therefore, these data must be considered as a "double-attenuated" measure through the atmosphere.

As one would expect, as the distance of atmospheric rain in which the light energy must travel increases, the percentage of transmitted light decreases. Some variability in the measurement results was seen which may be a result of the uncertainty associated with the rainmaking and the influence of the wind on the rain event. Further research would need to be conducted in order to investigate the impact of the rain making on the uncertainty.

Also of interest are the VTTI results of percentage transmission that exceed expected levels. For example, contrary to expectation, some illuminance measurements in rain conditions were greater than measurements in clear conditions. One possible explanation for such an

occurrence would be internal reflection as well as redirection of light through the rain. As an example, energy, that when unobstructed would pass beyond a target, may actually become redirected through water droplets and incorporated into measurements. In such an instance, the illuminance or luminance of an object in the rain would then be greater than in the clear condition.

Luminance data collected in both portions of this study were conducted solely using vehicle headlamps as sources of light. Future research is recommended in order to investigate the role of overhead lighting on the capabilities of pavement markings in the rainy atmosphere. The reflection of overhead light off wet pavement markings and its actual intensity as it reaches the driver also becomes a consideration. In addition to this, the strength of the prediction of illuminance or luminance in such an atmosphere would also be of interest.

Another consideration is the use of multiple materials as targets. For the discussed portions of this study, relatively smooth materials were used as a basis for illuminance and luminance measurements. Future investigations into differing materials and their respective retroreflectivity would be a possible area of interest.

Limitations

There are limitations or areas of error to be improved upon. For example, the measurement of illuminance may be a source for error. While every effort was made to ensure a consistent angle to the source of light, slight deviations toward or away from the road surface would result in an inaccurate measurement due to reflection of light from the road. Another source for error may be the use of the baffle. While decreasing the amount of reflection from the wet pavement to the illuminance meter, there may have been an increase in the internal reflection of light within the baffle device itself. Also of consideration is the sample size. While there was the ability to capture multiple rain rates, the size of the sample may be considered a limitation within each rain rate.

Conclusions

A correction of the amount of light energy that is actually transmitted through the rainy atmosphere was successfully developed. This correction applies to specified rain rates addressed in this study and provides an indication of how it may be applied to outside circumstances. Successful prediction of illuminance or luminance through the rainy atmosphere can now lead to

a greater understanding of the visibility of the pavement marking to a driver seeing the marking illuminated by light attenuated by headlamps.

It remains to be seen the extent to which the retroreflectivity of the targets addressed can be applied to realistic pavement markings. However, the preliminary steps to accurately addressing the retroreflectivity in a rainy atmosphere are compiled in the current report.

APPENDIX B: PROPOSED ALTERNATIVE CONTINUOUS WETTING TEST METHOD

The continuous wetting standard test method that was developed in part through this research has been proposed to ASTM Subcommittee E12.10 as WK19806. This proposed test method would serve as an alternate to E2176 (*5*). At the time of writing this report the final status of the proposed test method had not yet been determined. The authors feel that Test Method E2176 is only effective for pavement marking systems with optics having an index of refraction greater than 2.0, and/or structured markings having vertical structures greater than or equal to 3 mm. The proposed test method is a modified version of E2176. The modifications focus on a lower continuous wetting rate and a specific device to provide the wetting. The following describes the proposed test method.

EQUIPMENT

Retroreflectometer

- The retroreflectometer shall be an external beam instrument and shall be designed and constructed so that stray light will not affect the reading.
- The retroreflectometer shall meet the requirements of ASTM E1710 (*2*).

Spray Shield

- The retroreflectometer, if necessary, shall be modified with a rain/water shield to protect its lens from splattering rain/water during wet measurement.
- Adjust the shield such that it does not block the projected light and diminish readings. Determine area of marking being illuminated with the projected light. Adjust shield so that it does not cover any of this area and thus prevent complete wetting.
- The spray shield can also serve as the wind-shield to prevent wind from affecting the water spray pattern.

Rain Simulator (Continuous Wetting Apparatus)

The recommended rain simulator is defined by the following properties:

- A reservoir is needed for the water, preferably a portable backpack sprayer or other mobile reservoir with a capacity of at least 2 gallons.
    - It is essential that clean water shall be used. The spray nozzles are sensitive to debris in the water and in the water lines.
- The rain simulator shall have a battery-powered pump.
- The pump shall be regulated to control pressure as specified.
- A valve system shall be used to allow operation of two different nozzles independently.
- A wind-shield box shall be constructed to protect the spray from winds. The wind-shield box shall have dimensions adequately allowing the simulated rain to fall naturally while being lightweight and easy to handle for field applications.
- The wind-shield box shall have small cut-out openings on either end for a portable (handheld) external beam retroreflectometer to make measurements from.
- The wind-shield box shall have a feature to ensure proper measurement alignment.
- The rain simulator shall produce two continuous wetting rates such that the measured area uniformly receives 1 or 2 inches per hour of water (± 10 percent), respectively. Systems such as the TeeJet TX-1 and TeeJet TX-2 nozzles can uniformly and repeatably produce rates of 1 inch per hour and 2 inches per hour, respectively, over the measured area when oriented as specified below and operated at approximately 23 to 25 psi (however, other designs may be capable of producing the specified and uniform intensities of 1 and 2 inch per hour).[2]
    - With the wind-shield box having a width of 13 inches, length of 22 inches, and height of 30 inches, the face of the nozzles are located 8 inches from the bottom oriented 60 degrees up from horizontal (so the spray arcs up and then falls over the measurement area). It helps to have the nozzles on opposite ends of the wind-shield box.

Appendix C describes in detail the recommended rain simulator construction.

[2] The standardized pressure for the specific unit should be used to apply the desired wetting rate.

SAMPLING

The number of readings to be taken at each test location and the spacing between test locations shall be specified by the user. A minimum of four recorded measurements at each test location has been used in the past.

STANDARDIZATION

- The retroreflectometer shall be standardized using the instructions from the instrument manufacturer. A calibrated reference or working standard is used and is supplied with the instrument.
- Transporting the portable retroreflectometer from an air conditioned area to the test site may result in fogging of mirrors in the instrument. If there is any doubt concerning the standardization or if the readings of the reference or working standard are not constant, allow the instrument to reach ambient conditions and re-standardize with the reference or working standard.
- Verification must be made that there is no moisture on the retroreflectometer's lens when the instrument is being used for wet readings. Adjust the water protective shield as necessary.
- *Standardization Recheck* – If the subsequent readings on the reference standard deviate by more than 5 percent from the initial one, re-standardization shall be performed. If the readings on the calibrated reference standard deviate by more than 10 percent from the initial one, re-standardize and, in addition, re-measure previous measurements.

Continuous Wetting Rate Standardization

- To ensure that the correct amount of water is being continuously applied to the pavement marking, testing shall be performed to determine the actual output of the rain simulator. Either the scale method or depth method should be used to determine the continuous wetting rate. The operating pressure shall be adjusted until the desired wetting rate is achieved.
- Scale Method – This method requires a precise scale to weigh the water as it is collected on the pavement marking sample in the measurement area for a

predetermined amount of time. A container measuring 4-inches wide by 12-inches long shall be used to collect a sample of the continuous wetting. The weight of the water collected shall be 13.1 grams ± 10 percent per minute of run time for the 1 inch per hour rate and 26.2 grams ± 10 percent per minute of run time for the 2 inch per hour rate. The wetting shall run at least two minutes during testing.

- Depth Method – This method requires a ruler with a scale with enough resolution to accurately measure the depth of the collected water. A flat bottomed container measuring 4-inches wide by 12-inches long shall be used to collect water during the testing. The depth of the water collected shall be multiplied by 60 and divided by the length of the run time in minutes to determine the wetting rate. The wetting rate shall be within 10 percent for both the 1 inch per hour and the 2 inch per hour wetting rates. A minimum of a 10-minute run time shall be used.
- The wetting rate shall be checked daily to ensure the appropriate amount of water is being applied. If the spray pattern or rate changes, debris may have accumulated in the nozzles and that the wetting rate may no longer be within 10 percent of the desired level. The nozzles shall be cleaned, and the wetting rate rechecked.

GENERAL PROCEDURE

Both a dry and a wet measurement are usually taken in order to characterize the performance of the marking. The dry measurement establishes the effectiveness of the marking in a dry condition plus acts as a benchmark for the marking to which the wet performance can be compared. However, the dry measurement is optional per this test method.

Measuring Dry Retroreflectance

- Use the manufacturer's instructions for calibration and operation of the retroreflectometer.
- Locate the area of the pavement marking to be measured.
- Place the retroreflectometer squarely on the pavement marking material with the illumination in the direction of travel. Ensure that the illuminated measurement area of the retroreflectometer fits within the width of the stripe, and take a measurement.

Measuring Wet Retroreflectance

- With the retroreflectometer still in place, set the rain simulator in place and turn the water spray on to the specified level (1 or 2 inch per hour). Wet the marking to be measured for approximately 30 s to bring the marking into a saturation point. Begin to take measurements approximately every 10 s thereafter until little change in the values or a steady state condition occurs. This usually takes less than 30 s (or 60 s after the spray is turned on).
- NOTE: If measurements are made in a laboratory, then the markings sample shall be positioned with a two to three degree cross slope. If measurements are made in the field, the cross slope of the marking should be recorded. Measurements in the field shall not be made where water puddles and submerges the markings.
- Once steady state conditions have been reached, record a minimum of four measurements (unless specified otherwise) using the standard units of millicandelas per square meter per lux, ($mcd/m^2/lx$).

FACTORS THAT MAY INFLUENCE MEASUREMENTS

There are factors that may cause measurement variability when taking readings in the field. Some of these are:

- Slight changes in the position of the retroreflectometer on the marking may yield different readings.
- The rate of water spray.
- Wind can affect the water spray. A wind-shield must be used at all times.
- The ability of the water to wet the surface of the marking will affect the retroreflective readings. Newly installed pavement markings may have a natural surface chemistry which prevents wetting of the marking by rain/water. This phenomenon produces unreliable and unrepeatable results when measuring retroreflective efficiency under wet conditions. This non-wetting phenomenon is generally eliminated after one month of wear and weathering on the road. It is recommended to wait one month after installation to get a realistic value for the marking's performance.

- The longitudinal slope, and particularly the cross slope, of the roadway will influence the readings. More drainage (i.e., greater slope) can result in higher readings. Measurements should be made where the slope is representative of the roadway.

APPENDIX C: PORTABLE POWERED CONTINUOUS SPRAY SYSTEM FOR SIMULATED CONDITION OF CONTINUOUS WETTING DESIGN MANUAL

PARTS LIST

The parts list below contains all of the parts that were used in the construction of the Portable Powered Continuous Spray System detailed in this document. Where possible, generic parts are listed, but some specific vendor parts are listed. Care should be taken in selecting substitutions that meet similar capabilities to the specific parts.

Pressure System

Solo – Model 425 Backpack sprayer

Spraying Systems – 1/2 in. Pressure relief valve Model 23120

Sureflo – SLV10-AA46 Pump

Fluid filled pressure gauge (60 psi max)

Inline filter

Volt 12 Ah SLA AGM battery

Power switch

3/8 in. hose (use hose supplied with sprayer)

1/2 in. hose clamps

Material and hardware for pump and battery mounting

Parts in Figure 45

1. 1 in. female slip to 1 in. male threaded bushing
2. 1 in. male slip to 1/2 in. female threaded bushing
3. 1/2 in. street 90°
4. 1/2 in. street 45°
5. 1/2 in. x 4 in. nipple
6. 1/2 in. Pressure relief valve (listed above)
7. Gauge (listed above)
8. 1/2 in. threaded T
9. 1/2 in. male thread to 3/8 in. barb 90°

10. 1/2 in. male thread to 3/8 in. female threaded bushing
11. 3/8 in. male thread quick disconnect ***Note: for water not air*** (optional, can use fixed connection)

Measurement Box

1/4 in. male thread to 1/8 in. ferrule 90° (Grainger # 2P250)

1/4 in. threaded 90°

1/4 in. street 90°

1/8 in. ID plastic tubing for ferrule fittings (Grainger #)

Tee Jet – 1/4 in. nozzle housings CP8028-NYB

Tee Jet – nozzle cap CP8027-NYB

Tee Jet – tip strainer 8079-PP-50

Tee Jet – Cone Jet TX1 (1/2 iph)

Tee Jet – Cone Jet TX2 (1 iph)

Plexiglas for top

INTRODUCTION

This document details the construction of a prototype Portable Powered Continuous Spray System for use in simulating rain for continuous wet-retroreflectivity measurements of pavement markings. This system provided three relatively uniform and repeatable simulated rainfall rates of 1 and 2 inches per hour. The device consists of a backpack-mounted water storage system, battery-operated pump attached to the mount, and a handheld enclosed spray shroud. The following sections discuss the construction of the device, the calibration of the system, and the system operation.

CONSTRUCTION DETAILS

Figure 42 shows the standard backpack sprayer that was used in the construction. It originally consisted of the tank, support framing, spray wand, and pump lever. The latter two items, the spray wand and pump lever, were removed. Steps 1 through 5 detail the steps taken to construct the backpack sprayer, and Step 6 details the process of creating the spray box.

Figure 42. Standard Backpack Hand-Pump Sprayer.

Step 1: Remove Spray Wand

Remove the spray wand and pump lever from sprayer. If desired, the hose can be removed now for easier access, but do not discard this piece because it will be used later.

Step 2: Remove Pump Assembly

For the removal of the pump, the details below will be focused on this particular model. Remove the screw from pump cover at the bottom of the tank and slide the cover off (see Figure 43a). Then, remove two Allen head bolts from pump piston (see Figure 43b), and thread the pump body out of the tank. Remove bolt from the pump lever rod (see Figure 43c), and slide out the rod. The pump and the rod will not be used. Figure 43d is an image with the sprayer with pump and rod removed.

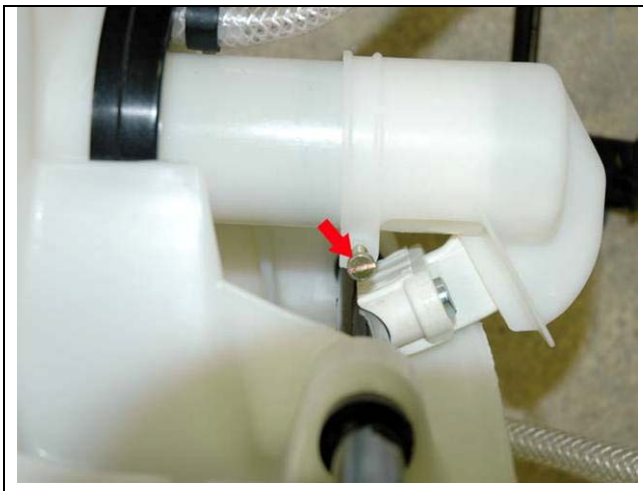

a) Remove pump cover screw.

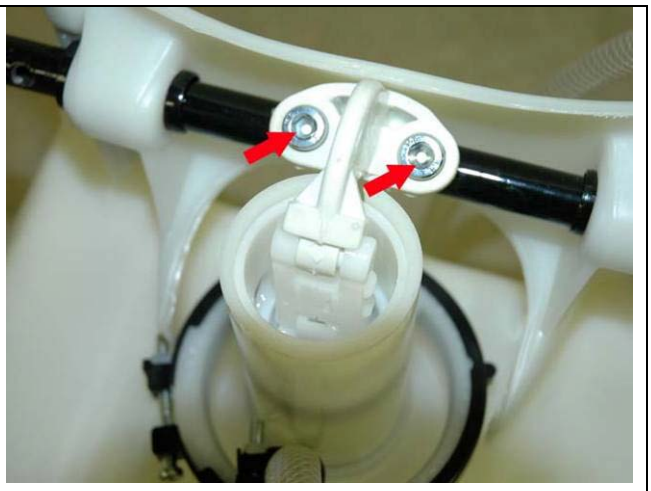

b) Remove pump piston screws.

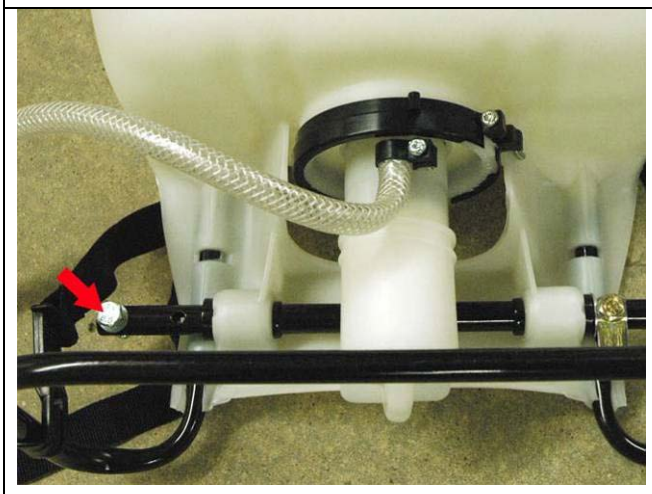

c) Remove pump lever rod bolt

d) Pump and lever removed.

Figure 43. Pump and Pump Lever Removal.

You will now need to open the storage tank and remove the pressure valve inside the storage tank (see Figure 44a). The black item on top of the tank in Figure 44b is the pressure valve for this model. You will not need it.

	
a) Top view of tank with pressure valve installed	b) Top view of tank with pressure valve removed

Figure 44. Pressure Valve Removal.

Step 3: Assemble Pressure Regulator

The pressure regulator is essential to providing a consistent, continuous, and repeatable spray application, so take care when assembling. All 11 parts of the pressure regulatory are shown in Figure 45a. Thread the 1 in. threaded bushing (#1) into the tank where the pump was removed. Use Teflon tape or other appropriate sealant. Assemble parts #2 thru #11 *before* attaching to part #1. The pressure valve and gauge will fit very close to the tank. If you do not like this arrangement the 4 in. pipe (#5) can be replaced with a longer one. Figure 45b is a depiction of the pressure regulatory attached to the storage tank.

Note: Dry fit and make sure all connections are tight and fit properly before gluing #2 bushing into #1 bushing. After the two bushings are glued up you will not be able to disassemble without cutting some parts.

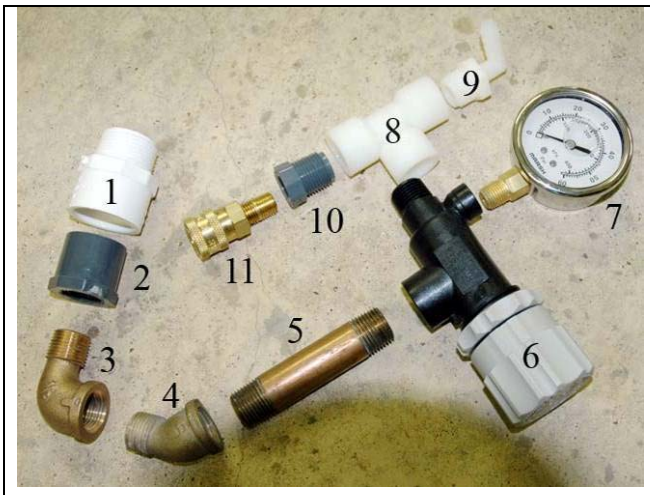

a) Pressure Regulatory Parts

b) Assembled Pressure Regulatory

Figure 45. Pressure Regulatory Assembly.

Step 4: Install Pump and Power

Install the pump and power supply. The pump and power supply need hard mounting points, so you will need to have mounting plates fabricated, such as the ones shown in Figure 46a. Then, you will need to place the appropriate mounting hardware that will enable the mounting plates to be attached to the backpack frame (see Figure 46b). In the next step, mount the pump, and attach lines and filter as shown in Figure 47.

Note: filter is directional and shown in the close-up image in the top left of Figure 47.

a) Fabricated mounting plates

b) Mounting tabs

Figure 46. Mounting Platform for Pump and Power Supply.

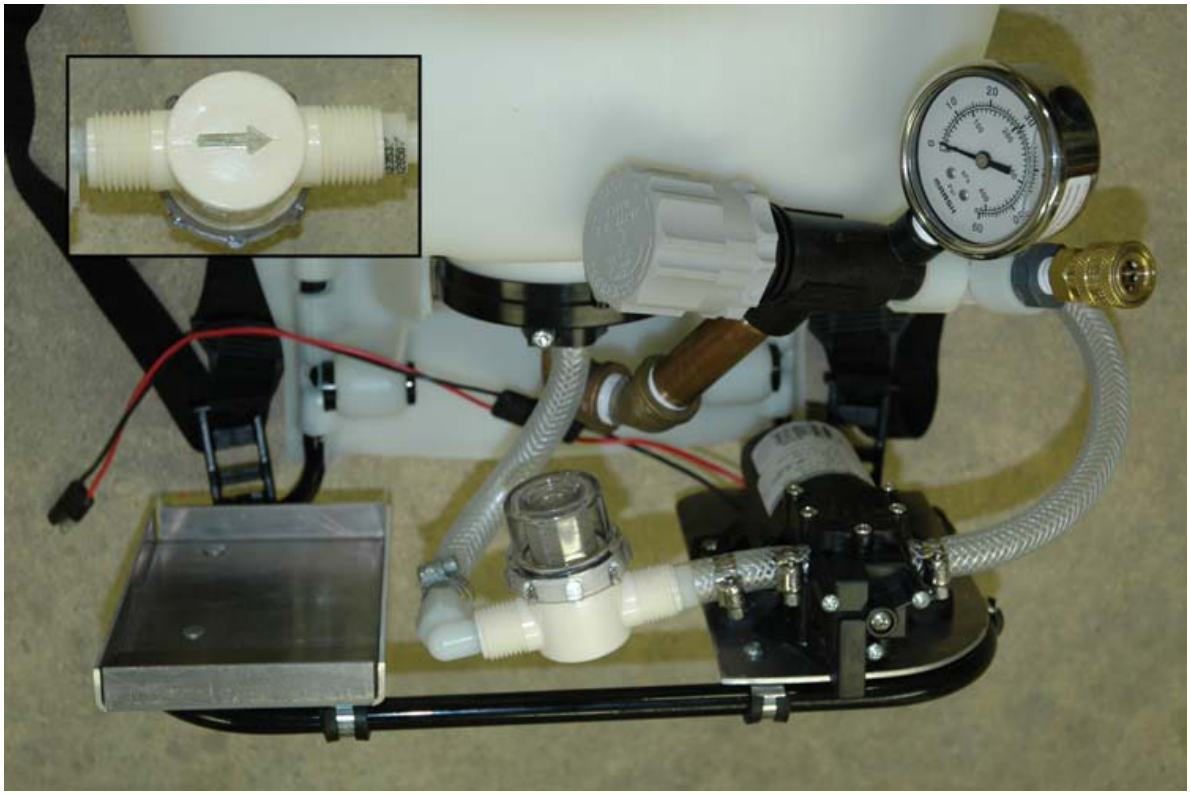

Figure 47. Mount Pump.

The final item to complete in this step is to install the power supply. Prior to installing the power supply, you will also need to fabricate a mounting bracket for a power switch. The power switch and its assembly are shown installed to the fabricated battery storage tray in Figure 48a. Figure 48b shows an image of the pump and power supply installed.

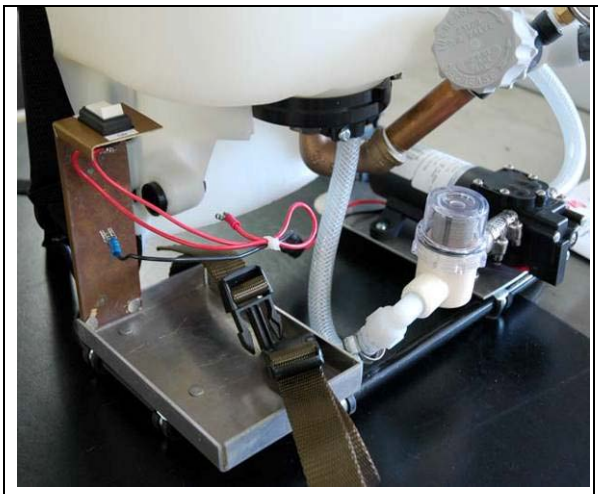

a) Switch and bracket

b) Pump and power supply installed

Figure 48. Power Supply Installation.

Step 5: Fabricate Spray Box

The majority of these components, with the exception of the spray nozzles, are generic. While there are other spray nozzles on the market, the ones detailed in this section are recommended based on experience. The dimensions detailed in Figure 49a are specific to the prototype, but could be modified with the understanding that the revised box should block out the prevailing wind, while providing ample room to allow for uniform spray distribution. The box should also be portable, yet rigid, and provide the appropriate access to make retroreflectometer measurements.

It is recommended to have the box fabricated out of sheet metal and preferable aluminum to minimize weight and rusting. Figure 49 contains an overhead image of the fabricated prototype spray box. Figure 49c shows a close-up of some of the rigid supports that were installed to ensure the stability of the spray box.

Next, the nozzles are assembled and installed. Figure 50 details the parts associated with the nozzles. The two different nozzles used in this prototype are depicted as #2a and #2b. It is important to note that the filter (#4) will help with minimizing debris clogging the nozzles, but it is recommended to use water with minimal sediment and to regularly clean and maintain the nozzles to ensure consistent operation. It is recommended to have 1 or 2 spare nozzles when in the field to minimize measurement delay.

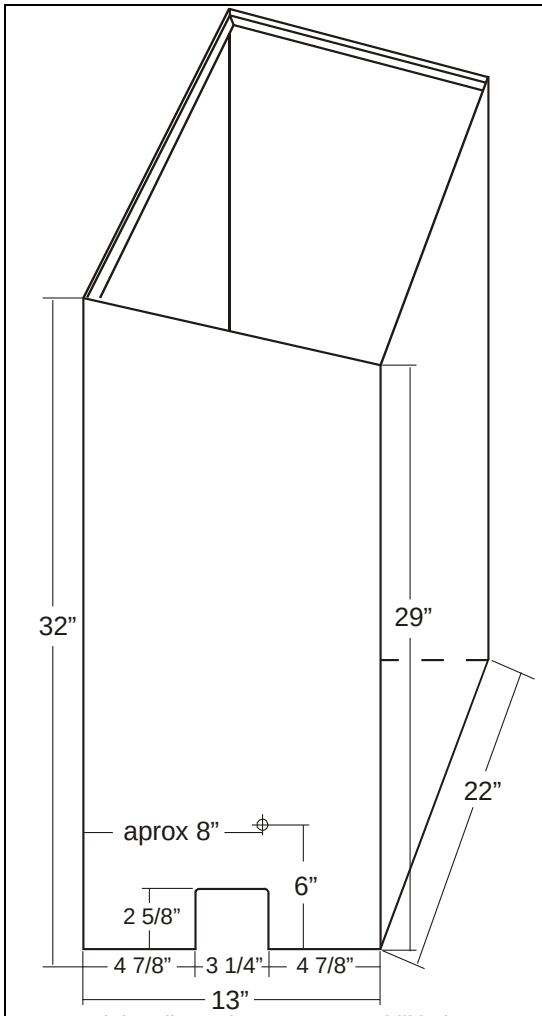

Note: Fitting dimensions may vary, drill hole so that nozzle is centered horizontally in end of box when mounted.

a) Dimensions

b) Top view

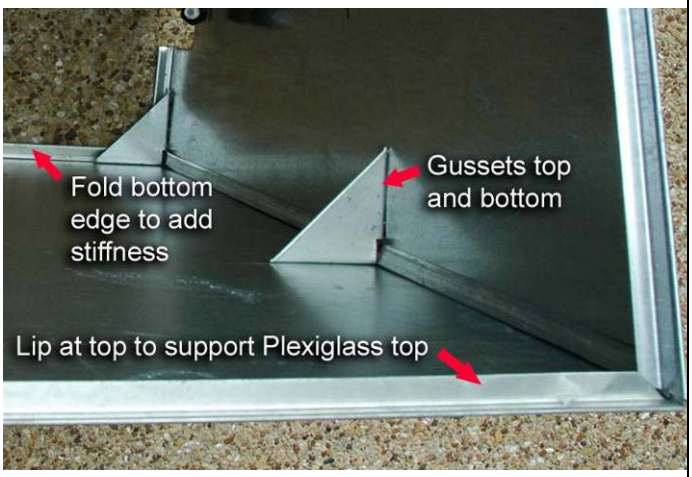

c) Close-up of rigid supports

Figure 49. Spray Box Design.

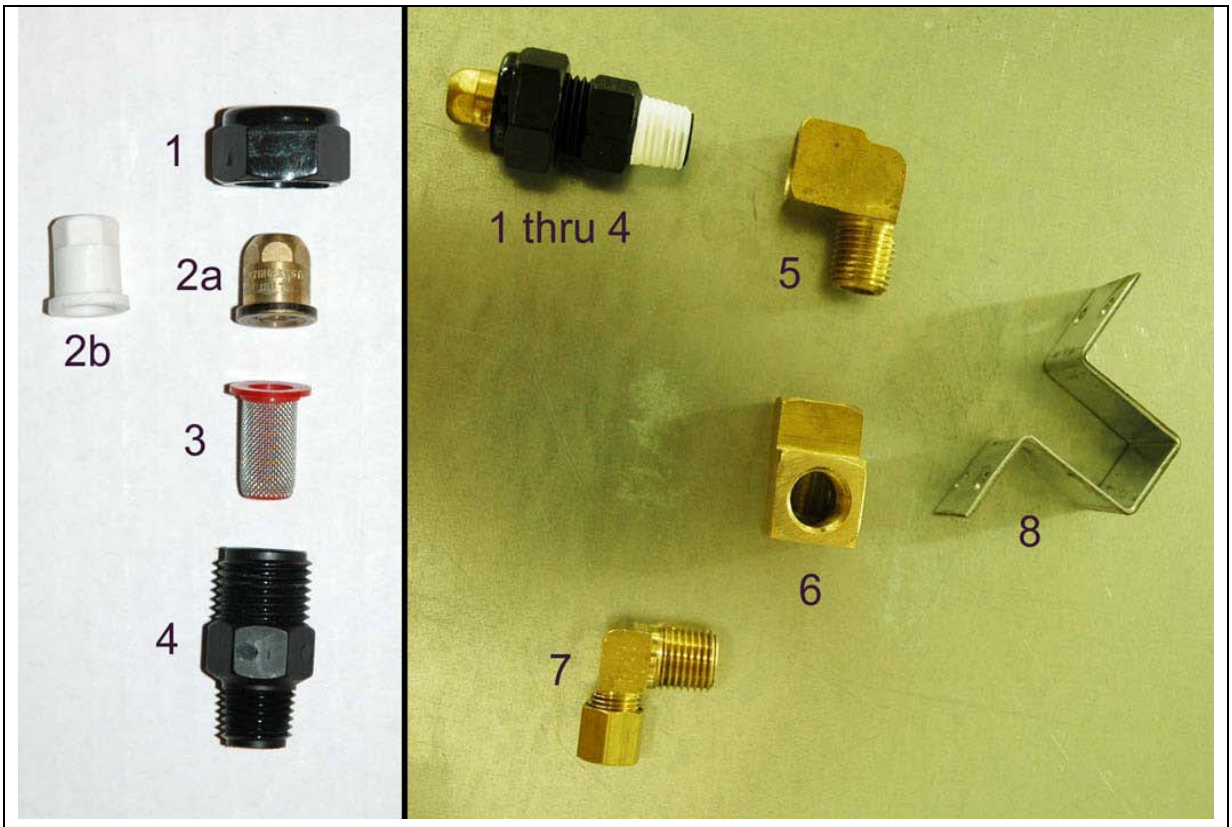

1) **Tee Jet** – nozzle cap CP8027-NYB
2a) **Tee Jet** – Cone Jet TX1 (1/2 iph)
2b) **Tee Jet** – Cone Jet TX2 (1 iph)
3) **Tee Jet** – tip strainer 8079-PP-50
4) **Tee Jet** – 1/4 in. nozzle housings CP8028-NYB
5) 1/4 in. street 90°
6) 1/4 in. threaded 90°
7) 1/4 in. male thread to 1/4 in. ferrule 90° (Grainger # 2P250)
8) Sheet metal bracket to hold #6 (have sheet metal shop bend)

Figure 50. Spray Nozzle Assembly

Once the nozzles are assembled, they are attached to the spray box. Figure 51 contains several pictures of the various points of interest with regard to the installation of the spray nozzles. Mount the nozzles (parts #1 thru #6 and #8 from Figure 50). The nozzle tip should be centered above the opening in each end of the box at approximately 8 inches from the bottom. This will require mounting the bracket slightly lower and offset from the center to achieve the proper nozzle tip location. The bracket should be mounted approximately 6 inches from the ground and approximately 8.25 inches from the side of the box. The nozzles will be aimed up

and toward the center of the box (see Figure 51b). Set the lower volume nozzle (TX1) 30° off vertical and the higher volume nozzle (TX2) to 25°. These settings should be adjusted during calibration of the system to ensure consistent and repeatable simulated rainfall within the measurement area. This particular prototype has two different spray nozzles and a 3-way water valve to control the flow of water to each of the nozzles. Figure 51c shows the 3-way valve. Figure 51d shows a top view of the completed spray box, which includes a Plexiglas lid to allow for viewing during testing. With the small aperture associated with each of the nozzles, it is also recommended to use a transparent lid to help check for clogged nozzles throughout testing. Figure 52 shows the completed prototype sprayer.

a) Exterior water line connection

b) Interior nozzle connection

c) Exterior water line directional valve

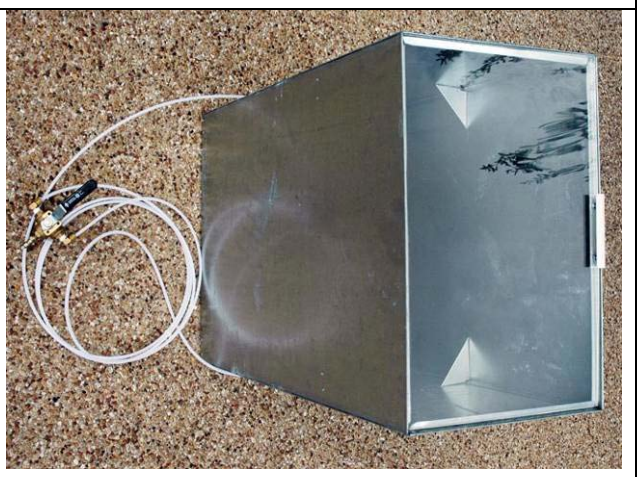

d) Completed spray box with Plexiglas lid

Figure 51. Spray Nozzles Installation.

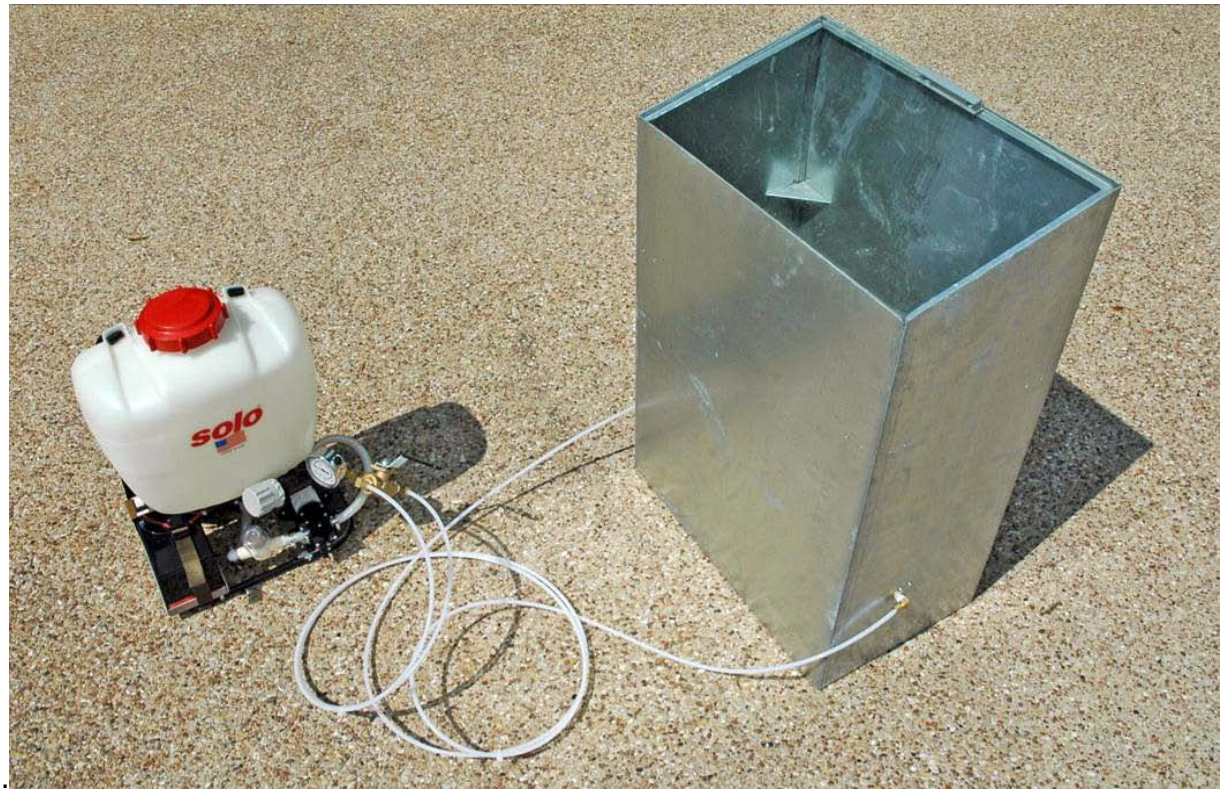

Figure 52. Completed Prototype Sprayer.

SYSTEM CALIBRATION

Calibration of the system is required to ensure the proper continuous wetting rate is being produced by each nozzle over the measurement area. The two important things to adjust during calibration are the angles of the nozzle tips and the pressure setting used for each of the two nozzles. As mentioned during the construction Step 5, the nozzles will be aimed up and toward the center of the box (see Figure 51b). Set the lower volume nozzle (TX1) 30° off vertical and the higher volume nozzle (TX2) to 25°. These angles should be used as the start point and adjusted up or down to control the angle of the spray to ensure that the water is distributed as evenly as possible across the measurement area. The start point for the pressure of the system should be between 23 and 25 psi. Each spray tip may require a different pressure to produce the exact amount of water desired. The TX1 nozzle should produce about half the amount of continuous wetting as the TX2 nozzle. Each nozzle should be run independently by using the valve to control the water flow. Operating both nozzles together may cause an uneven distribution of water across the measurement area.

To determine the appropriate nozzle angles and pressures several trials of the system should be conducted until the desired results are achieved. The most accurate way to measure the continuous wetting rate is to measure the weight of collected water within the measurement area. A shallow container of known area placed within the measurement area is the best method to collect the water. A container measuring approximately 4-inches wide by 12-inches long would be appropriate for most retroreflectometer measurement areas. It is recommended to check the system periodically to make sure that it is still producing the same continuous wetting rates.

SYSTEM OPERATION

The spray system should be operated in accordance with the ASTM standard test method for measuring the coefficient of retroreflected luminance of pavement markings in a standard and representative condition of continuous wetting. When operating the system, it is best to use the higher continuous wetting rate first as it will wet the marking area faster than the lower rate. When changing between rates it is best to allow sufficient time for the marking to adapt to the new wetting rate.

Always make sure that sufficient water is in the reservoir so that air does not get into the lines and impact the wetting rate. Also be sure to observe the spray pattern to make sure everything is properly aligned and that any obstructions have not entered the nozzles or water lines. Periodic calibration of the system is recommended to ensure that a similar continuous wetting rate is being applied.

APPENDIX D: RETROREFLECTIVITY DATA COLLECTION SHEETS

Table 8. LTL-Y Dry Retroreflectivity and Nighttime Chromaticity Data Collection Sheets.

LTL-Y Calibration			
Block/ Position	G Innermost	B Middle	R Outermost
Zero	1	6	5
White	2	3	4
Dark Yellow	7	8	9
Yellow	10	11	12

LTL-Y Dry Retroreflectivity and Nighttime Chromaticity		
1 = zero calibration 2 = R_L calibration 3-12 = readings	**Test Section:**	
	Direction:	
	Date:	
	Time:	

Yellow Edgeline Measurements			
Number/ Position	G Innermost	B Middle	R Outermost
1			
2			
3			
4			
5			
6			
7			
8			
9			
10			
11			
12			
13			
14			
15			
16			
17			
18			
19			
20			
21			
22			
23			
24			
25			
26			
27			
28			
29			
30			
31			
32			

White Lane Line Measurements			
Number/ Position	G Innermost	B Middle	R Outermost
1			
2			
3			
4			
5			
6			
7			
8			
9			
10			
11			
12			
13			
14			
15			
16			
17			
18			
19			
20			
21			
22			
23			
24			
25			
26			
27			
28			
29			
30			
31			
32			

Table 9. LTL-Y Dry Retroreflectivity and Nighttime Chromaticity Data Collection Sheets (Cont.).

LTL-Y Calibration			
Block/Position	G Innermost	B Middle	R Outermost
Zero	1	6	5
White	2	3	4
Dark Yellow	7	8	9
Yellow	10	11	12

LTL-Y Dry Retroreflectivity and Nighttime Chromaticity		
1 = zero calibration 2 = R_L calibration 3-12 = readings	**Test Section:**	
	Direction:	
	Date:	
	Time:	

White Edgeline Measurements			
Number/Position	G Innermost	B Middle	R Outermost
1			
2			
3			
4			
5			
6			
7			
8			
9			
10			
11			
12			
13			
14			
15			
16			
17			
18			
19			
20			
21			
22			
23			
24			
25			
26			
27			
28			
29			
30			
31			
32			

Table 10. BYK-Gardner Color-Guide Daytime Chromaticity Data Collection Sheets.

BYK-Gardner Color-Guide Daytime Chromaticity	
Test Section:	
Direction:	
Date:	
Time:	

Yellow Edgeline Measurements			
Number/Position	Y	x	Y
-			
1			
-			
2			
-			
3			
-			
4			
-			
5			
-			
6			
-			
7			
-			
8			
-			
9			
-			
10			
-			
11			
-			
12			
-			
13			
-			
14			
-			
15			
-			
16			

White Lane Line Measurements			
Number/Position	Y	x	Y
-			
1			
-			
2			
-			
3			
-			
4			
-			
5			
-			
6			
-			
7			
-			
8			
-			
9			
-			
10			
-			
11			
-			
12			
-			
13			
-			
14			
-			
15			
-			
16			

Table 11. BYK-Gardner Color-Guide Daytime Chromaticity Data Collection Sheets (Cont.).

BYK-Gardner Color-Guide Daytime Chromaticity	
Test Section:	
Direction:	
Date:	
Time:	

White Edgeline Measurements			
Number/Position	Y	x	y
-			
1			
-			
2			
-			
3			
-			
4			
-			
5			
-			
6			
-			
7			
-			
8			
-			
9			
-			
10			
-			
11			
-			
12			
-			
13			
-			
14			
-			
15			
-			
16			

Table 12. LTL-X Recovery Retroreflectivity Data Collection Sheets.

LTL-X Recovery Retroreflectivity	
Test Section:	
Direction:	
Date:	
Time:	

Yellow Edgeline Measurements	
Number	R_L
1	
2	
3	
4	
5	
6	
7	
8	
9	
10	
11	
12	
13	
14	
15	
16	

White Lane Line Measurements	
Number	R_L
1	
2	
3	
4	
5	
6	
7	
8	
9	
10	
11	
12	
13	
14	
15	
16	

White Edgeline Measurements	
Number	R_L
1	
2	
3	
4	
5	
6	
7	
8	
9	
10	
11	
12	
13	
14	
15	
16	

Table 13. LTL-X Continuous Wetting Retroreflectivity Data Collection Sheets.

LTL-X Continuous Wetting Retroreflectivity	
Test Section:	
Direction:	
Date:	
Time:	

Yellow Edgeline Measurements			
Number	0.8 iph	2.1 iph	9.5 iph
1			
2			
3			
4			
5			
6			
7			
8			
9			
10			
11			
12			
13			
14			
15			
16			
17			
18			
19			
20			
21			
22			
23			
24			

White Lane Line Measurements			
Number	0.8 iph	2.1 iph	9.5 iph
1			
2			
3			
4			
5			
6			
7			
8			
9			
10			
11			
12			

Table 14. LTL-X Continuous Wetting Retroreflectivity Data Collection Sheets (Cont.).

LTL-X Continuous Wetting Retroreflectivity	
Test Section:	
Direction:	
Date:	
Time:	

White Edgeline Measurements			
Number	0.8 iph	2.1 iph	9.5 iph
1			
2			
3			
4			
5			
6			
7			
8			
9			
10			
11			
12			
13			
14			
15			
16			
17			
18			
19			
20			
21			
22			
23			
24			

APPENDIX E: HANDHELD RETROREFLECTIVITY DATA

Table 15. Retroreflectivity Data for All Conditions.

Test Section	Measurement Condition	Average Retroreflectivity (mcd/m^2/lux)			Standard Deviation of Retroreflectivity Readings		
		Yellow Edgeline	White Lane Line	White Edgeline	Yellow Edgeline	White Lane Line	White Edgeline
1	Dry	191	156	216	26	24	27
	Recovery	220	104	160	24	19	39
	Continuous Wetting 0.8 iph	247	96	154	41	7	30
	Continuous Wetting 2.1 iph	216	83	134	39	9	26
	Continuous Wetting 9.5 iph	104	56	61	20	12	11
2	Dry	353	687	280	38	113	56
	Recovery	239	342	65	36	77	36
	Continuous Wetting 0.8 iph	190	256	42	20	67	24
	Continuous Wetting 2.1 iph	146	186	30	22	16	17
	Continuous Wetting 9.5 iph	103	184	40	16	33	8
3	Dry	153	185	217	18	14	22
	Recovery	103	221	135	35	26	38
	Continuous Wetting 0.8 iph	94	213	167	39	25	41
	Continuous Wetting 2.1 iph	79	179	117	38	22	47
	Continuous Wetting 9.5 iph	54	85	47	12	7	20
4	Dry	333	425	298	21	77	91
	Recovery	169	221	152	16	30	47
	Continuous Wetting 0.8 iph	166	215	138	11	9	34
	Continuous Wetting 2.1 iph	154	200	131	10	8	31
	Continuous Wetting 9.5 iph	116	159	109	8	6	26
5a	Dry	314	290	393	35	37	58
	Recovery	267	230	262	57	32	35
	Continuous Wetting 0.8 iph	288	233	232	55	11	21
	Continuous Wetting 2.1 iph	237	194	190	69	26	24
	Continuous Wetting 9.5 iph	124	103	89	50	31	18
5b	Dry	530	633	380	62	138	146
	Recovery	487	371	217	82	79	109
	Continuous Wetting 0.8 iph	481	427	188	56	7	155
	Continuous Wetting 2.1 iph	345	266	131	72	27	113
	Continuous Wetting 9.5 iph	241	172	62	39	38	34
6	Dry	215	295	402	12	28	61
	Recovery	30	73	42	7	19	18
	Continuous Wetting 0.8 iph	29	138	56	9	32	17
	Continuous Wetting 2.1 iph	25	109	37	8	33	15
	Continuous Wetting 9.5 iph	30	46	31	10	16	8
9	Dry	329	498	611	23	36	91
	Recovery	168	258	402	12	25	57
	Continuous Wetting 0.8 iph	176	279	320	16	27	84
	Continuous Wetting 2.1 iph	164	260	289	11	24	64

Test Section	Measurement Condition	Average Retroreflectivity (mcd/m^2/lux)			Standard Deviation of Retroreflectivity Readings		
		Yellow Edgeline	White Lane Line	White Edgeline	Yellow Edgeline	White Lane Line	White Edgeline
	Continuous Wetting 9.5 iph	134	216	250	12	33	66
11	Dry	174	199	235	47	20	35
	Recovery	85	46	62	31	14	16
	Continuous Wetting 0.8 iph	69	-	74	28	-	14
	Continuous Wetting 2.1 iph	53	-	61	23	-	13
	Continuous Wetting 9.5 iph	30	-	35	10	-	10
12	Dry	437	529	523	21	34	46
	Recovery	86	110	59	21	34	29
	Continuous Wetting 0.8 iph	54	-	59	16	-	23
	Continuous Wetting 2.1 iph	36	-	41	12	-	21
	Continuous Wetting 9.5 iph	19	-	24	4	-	10
14	Dry	361	424	586	17	40	45
	Recovery	53	45	86	17	12	46
	Continuous Wetting 0.8 iph	35	45	46	10	9	23
	Continuous Wetting 2.1 iph	19	31	45	4	11	27
	Continuous Wetting 9.5 iph	12	19	16	2	4	3

APPENDIX F: CCD PHOTOMETER EVALUATION DATA

Table 16. All Data from CCD Photometric Evaluation.

White Edgeline Average Values					Yellow Edgeline Average Values				
Section	Condition	Luminance (cd/m^2)	Retro (R_L)	Illuminance (lux)	Section	Condition	Luminance (cd/m^2)	Retro (R_L)	Illuminance (lux)
1	Dry	4.76	207	23.13	1	Dry	2.53	221	11.53
	Low	2.84	125			Low	2.62	233	
	Medium	2.41	106			Medium	2.33	207	
	High	1.51	66			High	1.62	148	
2	Dry	7.22	326	21.90	2	Dry	3.54	379	9.38
	Low	1.72	78			Low	2.30	246	
	Medium	1.48	66			Medium	2.04	219	
	High	1.49	67			High	1.37	144	
3	Dry	3.30	161	20.50	3	Dry	1.86	161	11.64
	Low	2.36	115			Low	1.39	122	
	Medium	1.80	87			Medium	1.47	131	
	High	1.13	55			High	0.91	79	
4	Dry	3.57	286	12.58	4	Dry	3.68	364	10.09
	Low	1.58	126			Low	1.70	170	
	Medium	1.42	113			Medium	1.72	172	
	High	1.30	104			High	1.55	153	
5	Dry	3.38	239	14.07	5	Dry	3.96	397	9.84
	Low	2.07	154			Low	2.44	247	
	Medium	1.72	124			Medium	2.09	211	
	High	1.21	86			High	1.44	145	
6	Dry	1.55	387	4.03	6	Dry	2.47	210	11.78
	Low	0.35	89			Low	0.72	61	
	Medium	0.34	85			Medium	0.62	53	
	High	0.23	58			High	0.64	54	
9	Dry	2.47	672	3.70	9	Dry	6.20	390	16.24
	Low	1.09	294			Low	3.14	192	
	Medium	0.93	251			Medium	2.93	180	
	High	0.89	237			High	2.64	162	
11	Dry	0.56	261	2.18	11	Dry	1.66	188	9.17
	Low	0.32	147			Low	0.57	62	
	Medium	0.23	103			Medium	0.56	63	
	High	0.25	122			High	0.39	42	
12	Dry	9.74	512	19.52	12	Dry	3.18	398	7.82
	Low	1.40	73			Low	0.74	94	
	Medium	1.13	60			Medium	0.61	78	
	High	0.83	42			High	0.51	65	
14	Dry	17.26	705	26.00	14	Dry	7.19	426	17.47
	Low	2.54	104			Low	1.32	91	
	Medium	2.41	98			Medium	1.32	94	
	High	1.34	55			High	0.74	53	

APPENDIX G: COMPARISON OF MEASURED AND CALCULATED RETROREFLECTIVITY

Table 17. Measured and Calculated Retroreflectivity Comparison Data.

Section Number	Measurement Condition	CCD Calculated R_L		Handheld Measured R_L	
		White	Yellow	White	Yellow
1	Dry	207	221	216	191
	Low	125	233	154	247
	Medium	106	207	134	216
	High	66	148	61	104
2	Dry	326	379	280	353
	Low	78	246	42	190
	Medium	66	219	30	146
	High	67	144	40	103
3	Dry	161	161	217	153
	Low	115	122	167	94
	Medium	87	131	117	79
	High	55	79	47	54
4	Dry	286	364	298	333
	Low	126	170	138	166
	Medium	113	172	131	154
	High	104	153	109	116
5	Dry	239	397	386.5	422
	Low	154	247	210	384.5
	Medium	124	211	160.5	291
	High	86	145	75.5	182.5
6	Dry	387	210	402	215
	Low	89	61	56	29
	Medium	85	53	37	25
	High	58	54	31	30
9	Dry	672	390	611	329
	Low	294	192	320	176
	Medium	251	180	289	164
	High	237	162	250	134
11	Dry	261	188	235	174
	Low	147	62	74	69
	Medium	103	63	61	53
	High	122	42	35	30
12	Dry	512	398	523	437
	Low	73	94	59	54
	Medium	60	78	41	36
	High	42	65	24	19
14	Dry	705	426	586	361
	Low	104	91	46	35
	Medium	98	94	45	19
	High	55	53	16	12